The neotectonic architecture of Taiwan and its implications for future large earthquakes

J. Bruce H. Shyu[1,*], Kerry Sieh[1], Yue-Gau Chen[2], Char-Shine Liu[3]

1: Division of Geological and Planetary Sciences, California Institute of Technology, MC 100-23, Pasadena, CA 91125, USA

2: Department of Geosciences, National Taiwan University, Taipei, Taiwan

3: Institute of Oceanography, National Taiwan University, Taipei, Taiwan

* corresponding author, Phone: +1-626-395-6177. Fax: +1-626-395-1740.
E-mail: jbhs@gps.caltech.edu

Accepted by *Journal of Geophysical Research* on 2005/02/08

Abstract

The disastrous effects of the 1999 Chi-Chi earthquake in Taiwan demonstrated an urgent need for better knowledge of the island's potential earthquake sources. Toward this end, we have prepared a neotectonic map of Taiwan. The map and related cross-sections are based upon structural and geomorphic expression of active faults and folds both in the field and on shaded-relief maps prepared from a 40-meter-resolution DEM, augmented by geodetic and seismologic data. The active tandem suturing and tandem disengagement of a volcanic arc and a continental sliver to and from the Eurasian continental margin have created two neotectonic belts in Taiwan. In the southern part of the orogen, both belts are in the final stage of consuming oceanic crust. Collision and suturing occur in the middle part of both belts, and post-collisional collapse and extension dominate the island's northern and northeastern flanks. Both belts consist of several distinct neotectonic domains. Seven domains – Kaoping, Chiayi, Taichung, Miaoli, Hsinchu, Ilan and Taipei – constitute the western belt, and four domains – Lutao-Lanyu, Taitung, Hualien and Ryukyu – make up the eastern belt. Each domain is defined by a distinct suite of active structures. For example, the Chelungpu fault (source of the 1999 earthquake) and its western neighbor, the Changhua fault, are the principal components of the Taichung Domain, whereas both its neighboring domains – the Chiayi and Miaoli Domains – are dominated by major blind faults. In most of the domains, the size of the principal active fault is large enough to produce future earthquakes with magnitudes in the mid-7's.

Keywords: Taiwan, earthquakes, neotectonics, seismic hazard, orogeny.

Introduction

Throughout its brief recorded history, Taiwan has experienced many strong and destructive earthquakes [e.g., *Bonilla*, 1975, 1977; *Hsu*, 1980; *Cheng and Yeh*, 1989]. These are the seismic manifestation of several million years of orogeny [e.g., *Ho*, 1986; *Teng*, 1987, 1990, 1996] (Figure 1). The human response to high seismicity has been building codes that anticipate high probabilities of future strong shaking on the island. Nonetheless, the disastrous effects of the M_w 7.6 Chi-Chi earthquake of 1999 show that many damaging effects were not anticipated. Meters of slip on the Chelungpu fault generated remarkable scarps that sliced through more than 80 km of urban, agricultural, and fluvial landscapes [*Central Geological Survey*, 1999a, b; *Chen et al.*, 2002]. Folding produced impressive broad deformation of the ground surface and resultant large areas of damage [*Chen et al.*, 2001; *Kelson et al.*, 2001; *Lee et al.*, 2002]. Modeling of geodetic and seismic data showed that the specific geometries of the fault surfaces played an important role in the production of the patterns, durations and levels of seismic shaking and surface deformation [*Ma et al.*, 2000, 2001; *Ji et al.*, 2001].

Many of these co-seismic phenomena could have been anticipated accurately if the earthquake source had been known in advance of the earthquake. For example, the trace of the principal fault that produced the 1999 earthquake was clear from its geomorphic expression well before its 1999 rupture, but had not been used to map prior ruptures systematically [*Chen et al.*, 2002]. The basic subsurface geometry of the fault had been known for nearly two decades [e.g., *Suppe*, 1976, 1980a, b], but important details had not been investigated using the patterns of deformation of fluvial terraces along the fault. The same is true of several other destructive historical co-seismic ruptures in Taiwan, most notably those of 1935 and 1951. This demonstrates the practical need for better knowledge of the active structures of the island.

Our goal in this paper is both academic and practical. We wish to identify, describe and interpret the principal active structural elements of Taiwan. For those interested in the evolution of the orogen over the past few million years, the current configuration of active structural elements is arguably the most accessible and complete piece of the puzzle, because so much of the older record has been eroded or buried [*Gilbert*, 1890, p.1]. On the more practical side, those interested in forecasting the effects of future fault ruptures must understand the locations, forms, and sense of slip of the active faults of the island. Realistic estimates of the magnitudes and patterns of future seismic shaking also require such knowledge. Moreover, reasonable interpretations of deformations now being recorded by an extensive geodetic network will be made best in the context of a firm structural, stratigraphic and geomorphologic framework. And, finally, future land-use planning will be well served by maps of geologically recent surface faulting and folding, in combination with maps of other geologic hazards.

Taiwan is well poised for the synoptic neotectonic evaluation we describe below. For decades, geographers have been mapping deformed fluvial and marine coastal terraces. More recently, radiometric dating of some of these surfaces have enabled determination of rates of latest Pleistocene and Holocene deformation. Concurrent with these geomorphic efforts, stratigraphers and structural geologists have been mapping the surface and subsurface configurations of young sediments, faults and folds and employing these to interpret the Neogene history of the Taiwan orogen. For the most part, however, these geomorphologic, stratigraphic and structural studies have not been applied to interpreting the youngest active structures of the island, nor have they been systematically integrated into a synoptic neotectonic map.

A vigorous debate is currently underway in Taiwan regarding the appropriate means by which to construct neotectonic maps. The disparate results of several recent attempts illustrate the controversy. Some have relied upon stratigraphic relationships that demonstrate Quaternary activity, believing that this is a sufficient basis for considering a fault to be active [e.g., *Shih et al.*, 1986; *Yang*, 1986]. Use of this criterion alone, however, is inadequate, since many faults that were active earlier in the Quaternary Period have been demonstrably inactive during the late Pleistocene and Holocene Epochs. At the other extreme are maps that depict as active only those faults that have ruptured historically [e.g., *H.-C. Chang et al.*, 1998; *Lin et al.*, 2000a]. These clearly are shutting the door after the horse has run out of the barn.

Our principal means for mapping the active structures of the island has been the use of fluvial and coastal landforms, which cover more than half of the surface of the island. Uplift and deformation of these features are readily apparent on shaded-relief maps. In many places, we have also utilized more detailed mapping of landforms published by others.

The recent availability of a high-resolution national Digital Elevation Model (DEM) makes the creation of a neotectonic map from landforms far easier than it would have been just a few years ago. Made from aerial photography of the island, the DEM has an elevation posting every 40 meters. Although standard stereographic aerial photographs have higher resolution and include tonal information, they are not geo-referenced, so the data derived therefrom are more difficult to compile and view. The 40-m DEM displays all major and most minor topographic features necessary for interpreting broadly the tectonic geomorphology of the island. Furthermore, high-resolution bathymetric databases that have recently become available [e.g., *Lallemand et al.*, 1997; *Liu et al.*, 1998; *Malavieille et al.*, 2002] allow us to incorporate geomorphic information from the surrounding sea floor.

Two examples clearly demonstrate the ability to identify most structures using the 40-m DEM (Figure 2). Topographic features along most segments of the Chelungpu fault, the source of the 1999 earthquake, revealed the exact location of not only all of the major ruptures, but also many of the secondary ones, even before the earthquake struck (Figure 2a). Another example, in the eastern part of Taiwan, shows that the topographic features visible in the DEM can be used to identify a major fault there, with its secondary folds and the different characteristics of the fault along several of its segments (Figure 2b). Due to space limitations, we can only include these two examples of the usefulness and our interpretations of the DEM data. High-resolution figures of interpreted DEM data for other part of Taiwan are available as electronic data supplements, along with much more detailed discussion of our interpretations.

Our primary reliance on the geomorphic manifestation of active structures means, of course, that we have undoubtedly missed some important features. For example, in the coastal plains where sedimentation rates are as high as 20 mm/yr [e.g., *Shyu*, 1999], surfaces that are deforming slowly may well be buried beneath late Holocene deposits. We have attempted to minimize this deficiency by incorporating locally available subsurface data. We may also have neglected to identify faults with low rates of slip within the high mountains, where rates of erosion are more than 5 mm/yr [e.g., *Hovius et al.*, 2000]. Furthermore, small features, such as the scarps that formed on the coastal plain during the historical earthquakes of 1906, 1935 and 1946, have been obliterated by human activity. We have relied on published post-seismic investigations of these historical ruptures to ensure that our map is as complete as possible. But this, of course, means that we are likely to have missed similar structures on the coastal plains that ruptured prior to the 20th century.

We have augmented our geomorphic analysis with as much additional stratigraphic and structural data as was available to us, to construct our map of the active tectonic features of the island. Even so, we do not claim to have made a complete description of the active structures of Taiwan. Decades of additional work would be required to accomplish that goal. Our intent has been simply to provide an up-to-date picture of the active neotectonic features of the island, compiled from sources of data currently available, and their implications for future large earthquakes.

Neotectonic overview of Taiwan

The island of Taiwan occupies a pivotal position along the boundary between the Eurasian and Philippine Sea plates. To the south, young Eurasian oceanic lithosphere of the South China Sea is subducting eastward beneath lithosphere of the Philippine Sea plate at a rate of about 80 mm/yr at the Manila trench [*Yu et al.*, 1999] (Figure 1a). To the north, by contrast, the polarity of subduction is the opposite, and extension is occurring at about 30-40 mm/yr in a back-arc region above the Ryukyu subduction zone [e.g., *Lallemand and Liu*, 1998].

The active Taiwan orogen embodies a tandem suturing and disarticulation [*Shyu et al.*, 2005a]. In southernmost Taiwan, consumption of Eurasian oceanic lithosphere is nearly complete, and two collisions are beginning (Figure 1a). On the west is the collision of a forearc sliver embedded within the Philippine Sea plate and the Eurasian continental margin. On the east is the collision of the forearc sliver and the Luzon volcanic arc [e.g., *Biq*, 1972; *Barrier and Angelier*, 1986; *Suppe*, 1987; *Reed et al.*, 1992; *Lundberg et al.*, 1992; *Huang et al.*, 1992, 1997; *Malavieille et al.*, 2002]. Taiwan consists of the rocks of these three lithospheric elements. Clastic sediments of the shallow-marine continental shelf constitute the western half of the island. Basement rocks and deep marine sediments of the forearc ridge form the island's high mountainous backbone. And volcanic rocks and associated marine sediments underlie the central eastern coast.

The Taiwan orogen is collapsing in the north and east, because of its transfer to the region of back-arc extension of the Ryukyu subduction zone [*Teng*, 1996; *Teng et al.*, 2000] (Figure 1a). The predominant feature of this back-arc region is the gaping Okinawa Trough, which has been opening to the south along the eastern flank of the island for the past few million years [e.g., *Suppe*, 1987; *Teng*, 1996]. This collapse in the north is chasing construction of the fold-and-thrust belt in the south and center.

Suppe [1981, 1984, 1987] calculated that the leading edges of both construction (in the south) and collapse (in the north) are both proceeding southward at about 100 mm/yr. Thus, latitude is commonly considered to be grossly correlative to orogenic maturity in Taiwan. Conventional wisdom is that if one wishes to understand what was happening in the north several Myr ago, one studies what is going on now in the ocean just south of the island.

The collapse of the orogen in the north is concentrated along the two sutures. The western suture is unstitching across the Okinawa Trough, which can be considered a reincarnation of the South China Sea. The eastern suture is tearing apart along the coastline a little farther south [*Shyu et al.*, 2005a] (Figure 1a). The disengagement of the western suture is clearly manifest in the oroclinal bending of the rocks of Taiwan's Central Range at the southern limit of current extension, where foliations of Central Range rocks bend eastward and strike out to sea, toward the Ryukyu island arc [e.g., *Tan*, 1977; *Suppe*, 1984]. Except for a right-lateral tear, no major structural break appears between the rocks of Taiwan's mountainous backbone and the westernmost part of the Ryukyu island arc. In fact, the oldest rocks of the southern Ryukyu Islands are metamorphic rocks that are similar to the Tananao Schists of the Central Range of Taiwan [e.g., *Kizaki*, 1986]. Thus, the Ryukyu arc next to Taiwan may well be the ancient forearc ridge of the Philippine Sea plate.

A similar disengagement of the eastern suture is apparent farther south, where the rocks of the Luzon arc in Taiwan's Coastal Range are pulling away from those of the forearc ridge (Central Range). Although we have no knowledge of the properties of the basement rocks between the Ryukyu arc and the trench, topography suggests that the old Luzon arc lithosphere overlies the shallower parts of the Ryukyu subduction zone [*Shyu et al.*, 2005a].

Taiwan thus provides a particularly clear example of the weakness of lithospheric sutures. The two sutures that juxtaposed three diverse pieces of lithosphere during collision only a few million years ago are being preferentially ripped apart now in the back-arc region of a subduction zone. This basic neotectonic framework of Taiwan will be important in making sense of its active tectonic structures, below.

Neotectonic domains of Taiwan

The Taiwan orogen consists of two principal loci of active deformation (Figures 1 and 3). On the west is a fold-and-thrust belt, along which shallow marine rocks of the outer continental shelf are piling up onto the Eurasian continental shelf of the Taiwan Strait. On the east is a second collisional belt, where the Luzon volcanic arc of the Philippine Sea plate is slamming into forearc rocks of the Central Range. Along both the eastern and western systems, collision began in the north about 5 million years ago [*Ho*, 1986; *Suppe*, 1987; *Teng*, 1987, 1990], reached the middle of the island about 3 million years ago [*Teng*, 1987, 1990], and is just beginning near Taiwan's southern tip [*Huang et al.*, 1992, 1997, 2000; *Kao et al.*, 2000]. In the process of double collision, most of the 300-km-wide piece of oceanic lithosphere between the Manila trench and the Luzon volcanic island arc has disappeared. Only the 40-km-wide strip of forearc-ridge lithosphere remains as the backbone of the island. The result has been a southward-progressing orogen.

Our examination reveals that the manifestation of active deformation varies considerably and progressively from south to north. However, this progressive along-strike variation in deformation is not gradational. Instead, it occurs across discrete steps. Hence, both the western and the eastern belts divide naturally into several distinct structural domains. Seven discrete domains comprise the western belt, and four constitute the eastern belt. Distinct principal structures characterize each of these eleven domains. Some domains are dominated by relatively simple emergent thrust faults, whereas others are dominated by hidden, or "blind," thrusts. In some domains the principal structures traverse tens of kilometers and cross the entire domain. In other cases, a myriad of small active structures prevail. The transitions between domains are well defined, although in several cases they are ten to twenty kilometers wide and involve the interpenetration of principal structures from the adjacent domains.

Below, we have divided our discussion into two sections, one for each of the neotectonic belts. In each section, we discuss the general characteristics of each of the eleven active structure domains. Each domain derives its name from the most prominent city or other geographic feature of the region. Due to space limitations, we have made more detailed discussion of these neotectonic domains, together with higher-resolution interpreted DEM figures, available as electronic data supplements.

Eastern neotectonic belt

The progressive south-to-north accretion and disengagement of the volcanic arc occurs across four discrete domains in eastern Taiwan. From south to north, collision is proceeding from the Lutao-Lanyu to the Taitung and Hualien Domains (Figure 3). These correspond to three stages in the accretion of the island arc—incipient collision, docking, and docked. Farther east and north, the Ryukyu Domain encompasses the splitting of the Coastal Range away from the Central Range and the locked part of the Ryukyu subduction interface.

The Lutao-Lanyu Domain is in the early stages of collision. A wide submerged fragment of forearc-basin lithosphere remains between the volcanic arc and the southeastern coast of the main island [e.g., *Huang et al.*, 1992]. GPS measurements show that it is being shortened at about 40 mm/yr (Figure 1b). This strain accumulation is accommodated by active thrust faults beneath the sea. To the north, in the Taitung Domain, forearc lithosphere has sundered completely and, except for shallow crustal sediments, is no longer visible at the surface. The volcanic island arc is accreting to the metamorphic core of the island at the prodigious rate of about 30 mm/yr along a suture marked by the narrow, north-south Longitudinal Valley (Figure 1b). Meanwhile, not only the forearc ridge has emerged above sea level, but the metamorphic core of the ridge has also risen to the surface as the major component of the Central Range. Farther north, in the Hualien Domain, lower geodetic rates of convergence suggest that accretion is nearing completion. Just north of the Hualien Domain, in the transition to the subduction of the Ryukyu Domain, the volcanic arc and forearc terranes are disengaging.

The bathymetry south of Taiwan is dominated by a prominent forearc ridge and forearc basin. This antiform/synform pair, the Hengchun Ridge and the Luzon Trough, strike roughly south-southeast, parallel to the trench and arc (Figure 1a). Bathymetric relief across these features is about 3 km, and together they span a forearc that is about 150 km wide. The Hengchun Ridge is the southward, submarine extension of the Hengchun Peninsula of southern Taiwan [e.g., *Huang et al.*, 1992; *Lundberg et al.*, 1997]. The Luzon Trough, between the ridge and the volcanic arc, does not extend onshore. Instead, it truncates against the southeastern coast of Taiwan, where volcanic arc rocks are first juxtaposed against the metamorphic rocks that form the basement core of the forearc. Thus, the oceanic lithosphere of the Luzon Trough must have been largely consumed in the course of southward progression of orogeny in Taiwan [e.g., *Chemenda et al.*, 1997].

Long ago, *Chen et al.* [1988] recognized that the submarine topography of the northern sector of the North Luzon Trough defines three north-south structural features. From east to west, these are the Taitung Trough, the Huatung Ridge, and the Southern Longitudinal Trough (Figure 4). The southern limit of the ridge and two troughs, at about 21.5˚ N, may demarcate the southern front of forearc shortening [e.g., *Huang et al.*, 1992, 1997, 2000]. The east-dipping Wadati-Benioff zone of the Manila trench, however, extends under these structures as far north as Taitung [*Huang*, 1997; *Kao et al.*, 2000]. This indicates that seismic deformation of subducting Eurasian oceanic lithosphere continues beneath the entire Lutao-Lanyu Domain but does not extend farther north (dashed black line in Figure 1a).

A closer examination of the structures within the Lutao-Lanyu Domain enables a better definition of the active structures of the incipient collision (Figure 4). The Huatung Ridge is probably an anticline or an anticlinorium. Seismic reflection lines show, in fact, that sediments on the western flank of the ridge at about 22˚20' latitude tilt westward [*Huang et al.*, 1992]. Bathymetry and seismic reflection profiles clearly show a west-dipping thrust fault on the east flank of the ridge from about 21˚40' to 22˚20'N [*Lundberg et al.*, 1997; *Chang et al.*, 2001; *Malavieille et al.*, 2002]. In the vicinity of 22˚N, a clear but lesser scarp exists on the west side of the ridge as well. North of about 22˚20'N, however, no scarps are obvious on either side of the ridge, so either the underlying thrust faults are blind or currently inactive. These observations and the basic symmetry of the Huatung Ridge suggest that it is the submarine expression of a fault-bend fold above a variably west-dipping thrust fault. Growth of the fold has been incremental, as evidenced by the presence of an antecedent meandering submarine channel cutting across the feature about halfway between the latitudes of Lanyu and Lutao islands (Figure 4).

High rates of uplift of the volcanic islands, about 3.4 mm/yr [*Chen and Liu*, 1992; *Chen*, 1993] since Late Pleistocene, suggest that the volcanic arc is also involved substantially in the incipient collision of the Lutao-Lanyu Domain. However, only one fault is obvious in the bathymetry: A 20-km long linear scarp west of Lutao (Figure 4) suggests that an east-dipping fault crops out there and dips under the island.

Recent geodetic measurements by GPS reveal that Lutao and Lanyu are converging northwestward toward the Hengchun Peninsula at about 40 mm/yr [*Yu et al.*, 1997, 1999]. We propose that slip on the major west-dipping thrust fault, on the east flank of the Huatung Ridge, accommodates most of this strain. The high uplift rates of Lutao and Lanyu islands suggest that thrust faults beneath them also are contributing significantly to the shortening. The high late Pleistocene uplift rates of these islands suggest that the component of horizontal shortening on the underlying thrusts is about 6 mm/yr, perpendicular to strike.

The northern edge of the Lutao-Lanyu Domain is abrupt. The Southern Longitudinal Trough, the Taitung Trough and the Huatung Ridge do not continue northward beyond the latitude of Taitung city (Figure 4). The submarine ridge of the volcanic arc disappears only a little farther north. The topography and bathymetry to the north is utterly different.

Figure 5 shows that the Taitung Domain is characterized by a long, narrow valley, between the Central Range and the arc-volcanic rocks of the Coastal Range, and a precipitous offshore escarpment. The active structures that have created these features are not contiguous with those of the Lutao-Lanyu Domain. In fact, the sense of vergence of the dominant structure changes abruptly across the boundary between the two domains.

The dominant neotectonic element of the Taitung Domain is the east-dipping Longitudinal Valley fault, along the eastern edge of the valley (Figure 5). It is characterized by high rates of sinistral reverse motion. A clear example of slip partitioning between strike-slip and dip-slip faulting occurs in the southern 20 km of the Taitung Domain [*J.-C. Lee et al.*, 1998; *Hu et al.*, 2001; *Shyu et al.*, 2002]. Geodetic measurements confirm that the Longitudinal Valley fault is active and slipping at a high rate. Across a segment of the Longitudinal Valley fault zone near Chihshang, creepmeters show that it is creeping obliquely at a high rate [*Angelier et al.*, 1997; *Lee et al.*, 2001]. Field measurements of deformed man-made structures indicate that the rate of horizontal shortening is about 22 mm/yr directed 323˚ [*Angelier et al.*, 1997], and leveling confirms a vertical dislocation rate of up to 20-24 mm/yr [*Yu and Liu*, 1989; *Yu and Kuo*, 2001].

Rupture of the Longitudinal Valley fault in the Taitung Domain produced two large earthquakes, three minutes apart, on 25 November 1951 — a M7.0 earthquake in the north, near Yuli, and a M6.2 earthquake in the south, near Chihshang [*Cheng et al.*, 1996]. The ruptures were not well documented, but there were sparse observations of fault rupture between about Chihshang and a point about 40 km north of Rueisuei [*Hsu*, 1962; *Cheng et al.*, 1996; *Shyu et al.*, 2005b] (Figure 5).

East-facing scarps on the seafloor about 50 km east of the Longitudinal Valley are evidence of active thrust faulting there. *Malavieille et al.* [2002] suggest that this fault is the principal fault of the Coastal Range block, and that the Longitudinal Valley fault is a back thrust that rises from it. We question the proposal that the Longitudinal Valley fault plays a subsidiary role, given its very high rate of slip. Such high rates suggest that the Longitudinal Valley fault is, in fact, the principal fault, and that the fault on the sea floor is subsidiary.

The existence of a reverse fault dipping westward beneath the eastern flank of the Central Range has long been suspected. *Biq* [1965], in fact, named this structure the Central Range fault. Several independent lines of evidence suggest its existence. First, the exposed slates of the Central Range formed at depths far below the land surface and, thus, must have been uplifted many kilometers. Second, the range's eastern flank is notably straighter than it is in the Hualien Domain to the north. Third, fluvial terraces are perched tens to hundreds of meters above modern streambeds along the eastern range front of the Central Range. Fourth, a leveling line that extends 16 km into the Central Range near Chihshang shows tilt of the easternmost 16 km of the range at about 0.8 μradian/year [*Liu and Yu*, 1990]. Similar eastward tilting of the eastern Central Range is also occurring west of the Yuli area [*Yu and Kuo*, 2001]. Furthermore, recent analysis of seismicity may support the presence of a west-dipping structure beneath the eastern Central Range [e.g., *Carena et al.*, 2001].

In summary, the principal structures of the Taitung Domain are accommodating about 40 mm/yr of obliquely convergent shortening (Figure 1b). Most of this is currently being taken up across the rapidly creeping (but occasionally seismic) Longitudinal Valley fault, which dips east beneath the Coastal Range. A subsidiary west-dipping reverse fault crops out about 40 km offshore, on the seafloor. The Central Range thrust, which dips under the eastern flank of the Central Range, also appears to be active.

At first glance, the northern half of the Longitudinal Valley does not appear to be all that different from the southern half (Figure 3). As to the south, the width of the valley is about 5 km (Figure 6) and it is filled with coarse clastic sediment derived predominantly from the Central Range on its western flank. Despite these similarities, the Hualien Domain (Figure 3) is fundamentally distinct from its neighbor to the south. The principal differences are that 1) the west-dipping Central Range thrust appears to be either inactive or much less active than it is to the south, 2) the east-dipping Longitudinal Valley fault has a higher ratio of sinistral to dip slip, and 3) rather than a west-dipping thrust fault offshore, the edge of the Ryukyu deformation front sits offshore.

Along the entire 65 km onland length of the Hualien Domain, the Longitudinal Valley fault crops out at the base of the western edge of the Coastal Range. Along much of that length, the fault has separate strike-slip and dip-slip strands. The strike-slip traces of the fault are much more prominent and continuous than they are in the Taitung Domain. The dominance of left-lateral movement on the northern Longitudinal Valley fault system near Hualien is also clear in geodetic measurements [e.g., *Chen*, 1974; *Yang*, 1999]. Seismic rupture of a section of the Longitudinal Valley fault provides additional support for the predominance of strike-slip over dip-slip. Rupture of the Meilun strand, which runs along the western edge of the Meilun Tableland near Hualien City, produced a M7.3 earthquake in October 1951 [*Yang*, 1953; *Hsu*, 1962]. Vertical offsets across the rupture were about 1.2 meters, and left-lateral offsets were about 2 meters [*Hsu*, 1955; *Lin*, 1957; *Bonilla*, 1975, 1977; *Yu*, 1997].

A submarine ridge extends northeastward approximately 10 km from the Meilun

Tableland (Figure 6). Further northeast is another submarine ridge, which trends nearly E-W and seems to be unconnected to any onland topography. The abrupt and steep scarps at its northern flank separate the ridge from the much lower and smoother Hoping Basin. These scarps appear to represent the initiation of the eastward peeling off of the Coastal Range from the Taiwan orogen. As one would expect in a region of transition between suturing and unsuturing, many minor structures are present in this area.

We find scant evidence for activity of the Central Range thrust within the Hualien Domain. The rarity of high lateritic fluvial terraces in the river drainages of the eastern flank of the range [*Yang*, 1986; *Chang et al.*, 1992] suggests lower uplift rates than to the south. Moreover, the sinuosity of the eastern flank of the Central Range indicates that rates of alluvial deposition outpace rates of uplift of the range. Thus it appears that the Longitudinal Valley fault is the only major active structure of the onshore part of the Hualien Domain.

The southern boundary of the Hualien Domain is well defined. It appears to be a 20-km-wide transition zone between Rueisuei and Kuangfu (Figure 6). At Rueisuei, the northernmost clear evidence for activity of the Central Range thrust is present. Between Rueisuei and Kuangfu, the geomorphology of the fault trace suggests that thrusting is dominant over sinistral slip, as in the Taitung Domain to the south. But we find no indication of activity of the Central Range thrust along this portion of the valley. Thus, this section of the valley is transitional between the two domains. Recent GPS measurements support this conclusion. They show that south of Kuangfu, the convergence rate normal to the strike of the Longitudinal Valley fault is as high as 30 mm/yr [*Yu et al.*, 1997, 1999]. North of Kuangfu, however, the convergence rate is dramatically lower – just 5 mm/yr.

The eastern and northern boundaries of the Hualien Domain are the edge of the Ryukyu subduction system. North of Hualien, the Coastal Range and Longitudinal Valley drop to sea level, and the sea laps against a precipitous eastern flank of the Central

Range (Figure 3). This is the southern edge of the extension associated with the Ryukyu subduction system and the tearing apart of the forearc/volcanic arc suture.

The Ryukyu Domain encompasses that part of the Ryukyu subduction megathrust nearest Taiwan that is capable of producing large subduction earthquakes. We have drawn the boundaries of the domain with the intention of encompassing all active structures between the trench and the southern side of the back-arc Okinawa Trough. The dominant structure in this domain is, of course, the subduction interface, but accommodation structures on the western edge of the domain are also important.

Isobaths drawn on the top of the Wadati-Benioff zone show that the dip of the Ryukyu subduction interface averages about 40˚ to a depth of about 50 km and steepens downdip from there to more than 55˚. The Wadati-Benioff zone defines the subducting slab to a depth of greater than 250 km [*Kao et al.*, 1998; *Kao and Rau*, 1999]. The termination of seismicity at the western edge of the Wadati-Benioff zone is abrupt. It trends nearly north-south, from the edge of the Ryukyu Domain to the western edge of the Taipei Domain (dashed black line in Figure 1a).

Secondary thrust faults in the hanging-wall block are also apparent. Immediately north of the Ryukyu trench is the Yaeyama forearc ridge [*Liu et al.*, 1998] (Figures 3 and 7), a 40-km-wide feature that consists of a series of E-W striking anticlinal ridges and synclinal valleys. Also, two major right-lateral faults in the northern portion of the ridge have been proposed to accommodate the oblique subduction direction [e.g., *Lallemand et al.*, 1999; *Chemenda et al.*, 2000; *Font et al.*, 2001]. North of this fold-and-thrust belt of the accretionary prism is an irregular 40-km- forearc trough that includes the Hoping and Nanao forearc basins [*Liu et al.*, 1998]. The southern flank of the trough is clearly faulted, with deformed and offset sediment layers in the seismic reflection profiles [e.g., *Schnürle et al.*, 1998; *Font et al.*, 2001].

The western margin of the Ryukyu Domain is a very complex transition zone between three domains: the Hualien, Ryukyu and Ilan Domains. Thus, in this region, one may expect to find numerous minor accommodation structures. Also, bathymetry shows that the westernmost part of the Ryukyu deformation front swings abruptly northward (Figure 7). The linearity of the scarp along this north-trending segment suggests a substantial component of right-lateral strike-slip. Two more right-lateral faults are present in the eastern part of the Hoping basin. On May 15th, 2002, a moderate earthquake (M_w = 6.0) resulted from slip on a related right-lateral strike-slip fault. The epicenter of the earthquake was offshore, about 25 km north of Nanao, and the fault plane solutions of the main shock and its aftershocks showed right-lateral movement on an approximately N-S striking plane. This structure is properly situated and oriented to serve as one of the structures that form the western boundary of the Ryukyu subduction zone.

Western neotectonic belt

Western Taiwan's active deformational belt divides naturally into seven distinct neotectonic domains. From south to north, these seven are the Kaoping, Chiayi, Taichung, Miaoli, Hsinchu, Ilan and Taipei Domains (Figure 3). As in the Eastern neotectonic belt, all but the northernmost represent a northward maturation in the progress of collision. As in the east, the northernmost domains encompass the region that has switched from shortening to back-arc extension of the Ryukyu subduction system. Unlike the Eastern neotectonic belt, however, the Western belt is not the result of volcanic arc/forearc collision and separation. Rather, it is the product of collision and separation of the forearc and the continental margin.

Docking of the two terranes begins in the southernmost (Kaoping) domain and disengagement occurs in the northern (Ilan and Taipei) domains. In the Kaoping Domain, deep-marine, shallow-marine and terrestrial sediments are deforming very rapidly by contraction and lateral extrusion over the last remnants of oceanic Eurasian lithosphere. Eurasian oceanic lithosphere continues to subduct beneath the entirety of this domain.

Along the central four domains of the Western belt, the lithosphere of the forearc ridge has made contact with the edge of the continental shelf, and shallow-marine and foredeep sediments of the continental shelf are being pushed northwestward farther onto the Eurasian continental margin. Very rapid rates of shortening continue to prevail in the Chiayi Domain, but the style of deformation is quite different than in the Kaoping Domain. There, a blind thrust fault system that extends out under the foothills and coastal plain predominates. Further north, in the Taichung Domain, rates of shortening are less, but two major emergent thrust faults, including the one that ruptured to produce the 1999 earthquake, dominate the neotectonic picture. Still farther north, across the Miaoli Domain, shortening rates are also relatively low, but the style of deformation is more complex; tight and open folds lie above a master blind thrust that extends from beneath the foothills all the way to the western coast. In Hsinchu, the next domain to the north, shortening is in its waning stages. Its active reverse faults trend more easterly than the strike of the western deformation belt and are cut by active strike-slip tear faults. Extension and subsidence characterize the active tectonics of the Ilan and Taipei Domains, the northernmost domains of the western belt. The Ilan Domain belongs to the western belt because it embodies the unstitching of the suturing that is currently in progress in the Kaoping Domain. It encompasses most of the back-arc extension of the Okinawa Trough. The Taipei Domain is dominated by a geologically minor normal fault in the hinterland of the Okinawa Trough. This one active normal fault lies on the western margin of the Taipei Basin and splits the edifice of the large, dormant Quaternary volcano to the north.

The Kaoping Domain, the southernmost of the western domains, encompasses the final episode of subduction of oceanic lithosphere prior to collision of forearc ridge and continental margin. Its northern boundary coincides with the northern limit of the

Wadati-Benioff zone of the Manila trench [e.g., *Huang et al.*, 1992; *Kao et al.*, 2000] (dashed black line in Figure 1a). It also coincides with the impingement of the Western Foothills and the Central Range, which we infer to reflect the elimination of oceanic lithosphere from between the edge of the Eurasian continental shelf and the forearc ridge. Unlike the more mature collisional domains farther north, the Kaoping Domain includes a rapidly subsiding basin, between the Central Range and the Western Foothills. We interpret this to be analogous to the submarine part of the Lutao-Lanyu Domain, its neighbor to the east: these are the last vestiges of oceanic lithosphere to be consumed prior to suturing (converging arrows in Figure 1a).

Both the submarine and subaerial sectors of the Kaoping Domain consist of three tracts. On the east is the forearc ridge, which continues onto land as the rapidly rising Hengchun Peninsula and Central Range (Figures 3 and 8). The peninsula and range consist of deep-marine turbidites and mélange in the south and metamorphosed slate and continental basement rocks in the north [e.g., *Chen et al.*, 1985; *Sung and Wang*, 1985, 1986; *Ho*, 1988; *Lin*, 1998]. This south-to-north progression of lithology indicates the progressive uplift and unroofing of the basement of the forearc ridge across the Kaoping Domain. On the western margin of the domain is a 50-km-wide submarine fold-and-thrust belt above the shallowest part of the Manila trench. This appears to extend onto land as the subaerial belt of deformation between Tainan and the Western Foothills. Between these eastern and western structural elements is a structurally non-descript tract of what must be marine lithosphere overlain mostly by deep-sea sediments. This extends onshore to the Pingtung Plain, where subsidence is occurring at rates up to 13 mm/yr in the Holocene [e.g., *Lu et al.*, 1998; *Shyu*, 1999].

The Chaochou fault separates the Pingtung Plain from the Central Range (Figure 8). The presence of Miocene-age rocks in the mountains on the east and a thick section of Quaternary strata in the basin to the west demonstrates that the fault has a significant component of vertical slip, up on the east [e.g., *Ho*, 1988]. The linearity of this fault suggests that it also has a significant component of strike-slip motion (Figure 8). Some previous mapping [e.g., *Wu*, 1978; *Ho*, 1988] inferred that this fault continues southward along the western front of the Hengchun Peninsula and becomes the Hengchun fault [e.g., *Shih et al.*, 1985; *Yang*, 1986] near the southern tip of the peninsula. Alternatively, *Malavieille et al.* [2002] suggest that the Chaochou fault runs southward into a submarine canyon west of the Hengchun Peninsula (Figure 3). The western flank of the Pingtung Plain may also represent another active fault.

Offshore to the southwest are numerous anticlinal ridges and minor thrust faults on the seafloor [e.g., *Liu et al.*, 1997] (Figure 8). Several submarine canyons cut through a series of these ridges, clearly indicating their antecedence and the incremental growth of the folds. We interpret this submarine fold-and thrust belt to be the result of the shortening of the forearc between the continental margin and the forearc Hengchun Ridge, and the embryonic form of Taiwan's Western Foothills.

On land, NE-SW striking right-lateral faults and N-S striking folds dominate the deformation of the Western Foothills (Figure 8). The orientations of these structures indicate an overall N-S stretching and E-W shortening of the shallow crust. The crust between these right-lateral structures and the two major left-lateral structures of the Pingtung Plain must be extruding southwestward [e.g., *Lacombe et al.*, 1999, 2001; *Chan et al.*, 2001, 2002].

In summary, deformation in the Kaoping Domain reflects E-W shortening and southward extrusion of sediments above a foundering oceanic lithosphere [e.g., *Lacombe et al.*, 1999, 2001]. This shortening reduces the width of the domain from more than 100 km in the south to less than 50 km in the north. With the shortening, a broad offshore fold and thrust belt in the south transforms into the nascent, narrow Western Foothills in the north, characterized by several prominent N-S trending folds and NE-SW trending right-lateral faults. Farther east, the rapidly-sinking Pingtung Plain is bounded by left-lateral structures that facilitate its southwestward extrusion, and is likely to be above the last piece of sundering South China Sea oceanic lithosphere.

Farther north, in the Chiayi Domain, the collision of forearc ridge and continental shelf has begun. There is no intervening basin analogous to the Pingtung Plain between the Western Foothills and the Central Range (Figures 3 and 9). Instead these two ranges abut along a fault zone that displays no clear evidence of activity. Furthermore, the Kaoping Domain's complex of small active folds and strike-slip faults within the Western Foothills does not extend northward into the Chiayi Domain. Rather, the folds of the Western Foothills there display no clear evidence for activity. Instead, the most prominent geomorphic evidence of youthful deformation exists in the low Chiayi Hills, farther west. Young lateritic fluvial terraces and active streambeds display evidence of recent folding along axes that trend nearly north-south. The geometry of these folds is broadly consistent with the presence of a shallow-dipping blind thrust fault complex beneath the Chiayi Hills and the coastal plain.

The low hills immediately west of the Western Foothills are commonly referred to as the Chiayi Hills. These hills are mantled with uplifted late-Quaternary lateritic fluvial terraces and consist of Quaternary fluvial sandstones and conglomerates. Between the Chiayi Hills and the west coast is the gently sloping Chianan Coastal Plain, the most important agricultural area in Taiwan. This basin is filled with Quaternary coastal and fluvial sediments up to 1500-2000 meters thick [*Stach*, 1958; *Hsiao*, 1971, 1974; *Sun*, 1970, 1971, 1972; *Tong and Yang*, 1999; *Yeh et al.*, 1999].

Bedrock structures east of the Chiayi Hills do not exhibit evidence of recent activity. In contrast, evidence for youthful tectonic deformation is abundant in the Chiayi Hills and the Chianan Coastal Plain (Figure 9). Uplifted fluvial terraces in the Chiayi Hills west of the Chukou fault clearly indicate deformation across several folds and minor faults [e.g., *Huang*, 1996; *Chen*, 1999]. Progressively tilted lateritic surfaces indicate ongoing deformation over the past few tens of thousands of years. Terraces along the major rivers of the Chianan Coastal Plain indicate regional uplift. This evidence belies the presence of a major active thrust fault below the Chiayi Hills and the Chianan Coastal Plain. This deeper structure has long been suspected [*Suppe*, 1980b; *Hung*, 1996; *Hung et al.*, 1999] and is likely to be the blind décollement of the western Taiwan fold-and-thrust belt. The deformation front associated with this blind structure, just a few kilometers inland from the west coast, is aligned with the deformation front of the Kaoping Domain, to the south. Small folds of the Chiayi Domain may be the result of irregularities in the underlying décollement and secondary structures above it [*Suppe*, 1976, 1980b]. Recent GPS measurements of the velocity field within the Chiayi Domain are consistent with the neotectonic evidence for a shallow blind master thrust fault [e.g., *Yu et al.*, 1997; *Yu and Chen*, 1998; *Hung et al.*, 1999; *Hsu et al.*, 2003].

The surface ruptures associated with two large destructive historical earthquakes provide important insights regarding the northern and southern boundaries of the Chiayi Domain. A M7.1 earthquake in 1906 occurred near the northern boundary of the domain, and was accompanied by right-lateral ruptures along the ENE striking Meishan fault [e.g., *Omori*, 1907; *Bonilla*, 1975, 1977; *Hsu and Chang*, 1979; *Huang et al.*, 1985] (Figure 9). Likewise, the southern few kilometers of the 1999 Chi-Chi rupture was a strike-slip fault that appears to be collinear with the 1906 Meishan rupture [*Central Geological Survey*, 1999a, b; *Lin et al.*, 2000b]. Therefore, the Meishan fault and the terminal right-lateral fault of the 1999 rupture serve as accommodation structures between the blind thrust décollement of the Chiayi Domain and the active thrust faults of the neighboring domain to the north.

Another historic fault rupture appears to have served a similar purpose at the southern end of the Chiayi Domain. This N70˚E rupture of the right-lateral Hsinhua fault produced the M6.8 earthquake in 1946 [*Chang et al.*, 1947; *Bonilla*, 1977] (Figure 9). Judging from its location, orientation and sense of slip, this structure is also likely to be an accommodation structure in the transition zone between the Kaoping and Chiayi Domains (Figure 3).

In the center of the western Taiwan orogenic belt, imbricated thrust sheets with many kilometers of accumulated slip reveal that the collision is well-established. Two sub-parallel thrust faults, the Chelungpu in the east and the Changhua in the west, are the major active components (Figure 10) of the Taichung Domain. These structures merge and die out near the southern edge of the domain and through a complex 20-km-wide transition zone in the north.

The 1999 rupture of the Chelungpu fault provided the critical first clue that the active Taiwan orogeny segregates naturally into discrete structural domains. The principal clue was that the fault broke along nearly the entire length of the active mountain front. Only along the ~90-km length of the 1999 rupture does the flank of the Western Foothills sport such a sharp, youthful, pre-existing thrust scarp [*Chen et al.*, 2002] (Figure 10). The length of this young scarp also coincides with the lengths of the Taichung piggyback basin and the tablelands to the west of the basin. The northern termination of the 1999 rupture occurred in a region where the structural and geomorphic expression of the thrust belt changes markedly [*Chen et al.*, 2000; *Lee et al.*, 2000]. North of the 1999 rupture, the tablelands dramatically change character and the Taichung foreland basin ends. All these observations indicate that there are fundamental structural differences between the portion of the Western Foothills and foreland basin adjacent to the rupture of 1999 and the regions to the north.

The other major active fault of the Taichung Domain underlies the Taichung Basin and the tablelands to the west (Figure 10). This fault bears several names in the literature [e.g., *Shih et al.*, 1983, 1984a, b; *Shih and Yang*, 1985; *Yang*, 1986], but is commonly referred to as the Changhua fault.

The tablelands are the geomorphic expression of the Changhua fault (Figure 10). Their surfaces and underlying Quaternary deposits form an anticlinal welt separating the Taichung and coastal foreland basins. Small steep west-facing scarps along the western flank of the Houli and Tatu Tablelands suggest that the Changhua fault breaks the surface, at least locally [*Pan et al.*, 1983; *Shih et al.*, 1983, 1984a, b; *Shih and Yang*, 1985; *Yang*, 1986]. Despite these steep scarps, several recent seismic reflection lines suggest that the Changhua fault itself may be a fault-propagation fold that does not break cleanly to the surface [*Lee et al.*, 1997; *Shih et al.*, 2000, 2002; *Yang et al.*, 2000; *Hsu*, 2001], as was suggested by *Chen* [1978]. Nonetheless, the presence of steep scarps suggests that deformation on the western flank of the tablelands could be severe locally during ruptures of the Changhua fault.

The Changhua fault appears to represent the western limit of active deformation at the latitude of the Taichung Domain. Thus, the western limit of deformation in the Taichung Domain is substantially farther to the east than it is in the neighboring Chiayi and Miaoli Domains (Figure 3). Total reverse slip on the Changhua fault is merely a few hundred meters [*Chen*, 1978], far less than the many kilometers of slip on the Chelungpu fault. However, the long-term slip rate and the age of initiation of the Changhua fault are unknown currently, so that the fraction of strain across the Taichung Domain that is taken up by the Changhua fault is not known. Nor have paleoseismic studies shed any light on the recurrence characteristics of the fault.

Both ends of the 1999 rupture provide important information about the transitions of the Taichung Domain with its neighbors to the north and south. In the south, geomorphic features indicate that both the Chelungpu fault and the Changhua fault diminish in prominence south of the Choushui River and terminate in the dextral strike-slip fault mentioned earlier (Figure 10). The geomorphic expression of the Chelungpu and Changhua faults also diminishes in this region. The Changhua fault probably extends along scarps on the east side of the Chinshui River valley and diminishes southward along this tributary river valley and merges with the Chelungpu fault as shown in Figure 10 [*Ota et al.*, 2002]. This interpretation suggests an overlap in structures of the Taichung and Chiayi Domains. Structures underlying the Touliu and Chiayi hills are the northernmost expressions of the Chiayi Domain, and the dying southern strands of the Chelungpu and Changhua faults south of the Choushui River are the southernmost expressions of the Taichung Domain. The overlap of these structures indicates that the transition between the two domains is about 20 kilometers wide (Figure 3).

Complexities at the northern end of the Taichung Domain define a wide transition zone with its northern neighbor, the Miaoli Domain. The odd, east-striking anticlinal welt and bounding thrust faults and kink bands that formed the ~10-km-long northern segment of the 1999 rupture [*Chen et al.*, 2001] form a small rabbit-ear-like anticline that cuts across regional bedding and into this syncline. Spectacular though this co-seismic welt was, it is not a large regional structure. The Chihhu syncline, across which this minor appendage of the 1999 rupture cut, is a major element of the Miaoli Domain to the north (Figures 10 and 11). This indicates that the northernmost rupture of the Chi-Chi earthquake is not really part of the Chelungpu fault; rather it is a surficial accommodation structure within the transition zone between the Taichung and Miaoli Domains.

A co-seismic fault rupture, associated with a large earthquake in 1935, is also within the transition zone between these two domains. The predominantly right-lateral Tuntzuchiao fault extends southwestward across the northern edge of the Taichung Basin into the Houli and Tatu Tablelands. It cuts across the strike of the basin and tablelands at about a 45˚ angle, about the relationship one would expect for a strike-slip structure serving as an accommodation structure within a fold-and-thrust belt [e.g., *Yeats et al.*, 1997]. The fault separates the tablelands to the south from the broad open Tunghsiao anticline and associated folds of the Miaoli Domain to the north (Figures 10 and 11). The width of the transition zone between the Taichung and the Miaoli Domains, as measured by the distance between the southern end of the Tuntzuchiao fault and the northern end of the Sanyi fault, is about 20 kilometers.

The active structures of the Miaoli Domain are roughly on trend but contrast sharply with those of the Taichung Domain (Figure 3). The active tectonic landforms on land are broad coastal and narrower foothill anticline-syncline pairs (Figure 11). Reverse faults, including one that ruptured during an earthquake in 1935, are locally clear in the topography. The fact that active folding extends to the west coast suggests that a west-verging master thrust fault underlies the entire region between the Western Foothills and the coast. GPS geodetic measurements show that convergence across the domain is approximately N40˚W at about 5 mm/yr [e.g., *Yu et al.*, 1997], similar in azimuth but far lower in magnitude than convergence across domains to the south.

The two major anticline-syncline pairs that dominate the landforms of the Miaoli Domain are along strike with the features of the Taichung Domain. The eastern pair, the Chuhuangkeng anticline and Chihhu syncline, forms the western flank of the Western Foothills (Figure 11). The Shihtan fault, a bedding-plane back-thrust on the steep eastern limb of the syncline, ruptured during the 1935 earthquake [*Hayasaka*, 1935; *Otuka*, 1936; *Wang et al.*, 1994]. The structural position of the Shihtan fault, on the limb of a syncline and parallel to bedding, indicates that it is not a major structure.

West of the Miaoli valley is the other pair of major folds, the Tunghsiao anticline and Tunglo syncline [e.g., *Chang*, 1974; *Chinese Petroleum Corporation*, 1994]. The geomorphic expression of this anticline is less clear than that of the Chuhuangkeng anticline, because only gently dipping, less consolidated young beds are exposed in its eroded core. Tilted remnants of a lateritic terrace west of the town of Sanyi form a prominent cap to the eastern limb of this anticline [e.g., *J.-C. Chang et al.*, 1998].

In contrast to the Taichung Domain, no major thrust fault crops out on land within the Miaoli Domain. Nonetheless, the two major anticline and syncline pairs probably are the superficial manifestation of a major underlying detachment [e.g., *Elishewitz*, 1963; *Suppe and Namson*, 1979; *Namson*, 1981, 1983, 1984; *Hung and Wiltschko*, 1993]. This major detachment, if it were to crop out at the surface, would do so offshore and delimit the western edge of the Miaoli Domain. In fact, previous seismic reflection surveys have found folds offshore of the Miaoli area [*Wang*, 1967], indicating that the detachment does indeed continue beneath the offshore region.

The fact that the deformation front of the Miaoli Domain is much farther west than that of the Taichung Domain suggests a structural down-step from the Changhua and Chelungpu faults of the Taichung Domain to the décollement of the Miaoli Domain [e.g., *Chen et al.*, 2001]. This step is accommodated by many minor structures in the transition zone between the two domains.

The Hsinchu Domain contains the northernmost evidence for active crustal shortening in Taiwan. It is a transitional domain between the active shortening of the Miaoli Domain and active extension of the Taipei Domain (Figure 3). Its reverse and strike-slip faults bring the active deformation front of the Miaoli Domain back onto land. N-S shortening across the domain is accommodated by two groups of reverse faults and folds. GPS measurements are not coherent across the Hsinchu Domain but do suggest that shortening rates are no more than a few mm/yr.

Two groups of active structures disrupt rocks of the foreland basin. The northern of the two groups of active structures disrupts the surfaces of the Taoyuan-Hukou Tableland as a series of ENE-WSW striking scarps and fold axes (Figure 12). The scarps have long been considered to be active fault or fold scarps [e.g., *Hanai*, 1930; *Ku*, 1963; *Sunlin*, 1982; *Yang*, 1986]. All of the scarps are related to two major structures, the Pingchen and Hukou anticlines [e.g., *Tang*, 1963; *Wang*, 1964]. The Hukou anticline is likely to be a fault-bend fold created by an underlying thrust ramp, and the higher scarp south of the valley is a manifestation of its forelimb. The Pingchen anticline appears to be the result of a wedge thrust, and the lower scarp north of the valley may be a fold scarp related to its forelimb [*Wang*, 2003]. A right-lateral fault zone that strikes WNW-ESE forms the southern boundary of the structures of the Taoyuan-Hukou Tableland [*Wang*, 2003]. The fact that this right-lateral fault zone heads offshore suggests that it is a tear fault between the structures of the Tableland and unidentified structures offshore.

The other group of active structures in the Hsinchu Domain is geomorphically apparent just south of the Touchien River (Figure 12). Scarps of the Hsincheng and Hsinchu faults and enigmatic intervening scarps cut and deform the narrow fluvial terraces south of the river. The overall trend of the fault system is east-west.

Both of the two groups of faults in the Hsinchu Domain accommodate shortening in a direction that is nearly north-south. Thrust faults that strike NNE dominate the domain, but right-lateral faults intersect these at angles of about 45˚ [e.g., *Yang et al.*, 1996, 1997]. The direction of shortening across these faults is NNW, nearly 80˚ clockwise from the direction of shortening across the Miaoli Domain.

This kinematic interpretation is consistent with the Hsinchu Domain being the northernmost region of shortening in Taiwan. To the south, the Miaoli Domain continues to suffer WNW-ESE shortening as a result of the collision of the forearc sliver of the Central Range and the South China continental shelf. To the north, the Taipei Domain is experiencing post-collisional collapse in the region of back-arc extension above the Wadati-Benioff zone of the Ryukyu subduction system [*Teng*, 1996; *Teng et al.*, 2000] (Figure 3). The neutral plane separating these two regimes is immediately north of the Hsinchu Domain. In this context it is reasonable to conclude that the structures of the Hsinchu Domain are merely the northern end of the structures associated with the major detachment of the Miaoli Domain, as suggested by *Biq* [1992]. However, bathymetric data offshore Hsinchu and Miaoli are insufficient to test this hypothesis [e.g., *Pan and Hu*, 1972].

Within the Taipei Domain, formerly active thrust faults are being buried by young fluvial, marine, and volcanic sediment and locally obliterated by the construction of a volcanic edifice. NW-SE extension across the domain is concentrated on one principal normal fault, across which the long-term rate of extension appears to be at least 1 mm/yr (Figure 13). Motion across this structure, the Shanchiao fault, has been producing the Taipei Basin half-graben for the past few hundred thousand years. Seismic slip on the fault may have produced a marine incursion into the Taipei Basin in 1694. Decadal rates of extension across the domain are poorly constrained by GPS measurements [*Yu et al.*, 1997], but the magnitude of extension could be consistent with the long-term rate of extension across the Shanchiao fault.

The major active structure of the Taipei Domain is the Shanchiao fault, which separates the Taipei Basin and the Linkou Tableland (Figure 13). The observation of numerous triangular facets along the eastern foothills of the Linkou Tableland led to the discovery of the fault many decades ago [*Tan*, 1939; *Lin*, 1957]. In general, the surface trace of the Shanchiao fault lies slightly east of the inactive Hsinchuang fault [*Sun*, 1990], a thrust fault that probably represents the deformation front of northern Taiwan in the early Quaternary Period [*Ho*, 1988; *Wang-Lee et al.*, 1978; *Teng et al.*, 2001]. The parallel traces of the two faults suggest that the steeper normal fault and shallower thrust fault merge at depth and that the younger Shanchiao fault has reoccupied the older fault plane [e.g., *Wu*, 1965; *Hsieh et al.*, 1992]. The reoccupation by the Shanchiao fault of the Hsinchuang fault in the late Quaternary Period demonstrates that the Taipei Domain has changed recently from a regime of shortening to one of extension. This is consistent with the movement of the domain out of the influence of the Manila subduction system to that of the Ryukyu subduction system [e.g., *Suppe*, 1984, 1987; *Teng*, 1996; *Teng et al.*, 2000].

The Tatun volcanic edifice is clearly bisected by the northern extension of the Shanchiao fault (Figure 13). On the uplifted block, northwest of the fault, the semi-circular perimeter of about half the edifice is preserved. Southeast of the fault, the narrower width of the volcanic construct may well be due to burial of the flanks by sediments of the Taipei Basin. In detail, the scarp across the volcano is not as clear as it is between the Taipei Basin and Linkou Tableland. Nonetheless the overall trajectory of the fault zone over the volcano is clear, and numerous small scarps and other linear features form a clear fault zone.

History records a very interesting occurrence that is quite relevant to understanding the relevance of the Shanchiao fault to seismic hazard assessment. In 1694, historical documents indicate an abrupt subsidence in the Taipei region, with the formation of a brackish-water lake that inundated at least a third of the basin [*Shieh*, 2000]. The lake was deep enough to permit large ships to sail far into the basin. The formation of the lake is most easily explained by several meters of slip on the Shanchiao fault, since such a rupture would result in subsidence of a large portion of the Taipei Basin.

The Okinawa Trough is the back-arc basin of the Ryukyu subduction system (Figure 1). Its progressive westward propagation is splitting the country's mountainous backbone along the western suture, now occupied by the Lanyang Plain (Figure 14). This large, triangular basin reflects the current foundering of the western tip of the westward propagating Okinawa back-arc trough. On the northwestern flank of the Lanyang Plain is the Hsueshan Range, and on the southern flank of the plain is the northern tip of the Central Range. Two observations suggest that these flanking ranges are sinking as well. First, their crests are appreciably lower than range crests farther south. Second, their flanks are being buried by alluvium on the east coast and in the Taipei Basin.

If *Suppe*'s [1987] calculation is correct that the western edge of Ryukyu subduction is migrating southwestward at about 100 mm/yr, then one would anticipate that none of the extensional features nor the sinking of the onshore part of the Ilan Domain would be older than about a half million years. This is supported by stratigraphic evidence that post-collisional collapse of northeastern Taiwan has occurred in just the past million years [*Teng*, 1996; *Teng et al.*, 2000].

Two systems of geomorphically expressed normal faults are apparent in the onland portion of the Ilan Domain. They bound the Lanyang Plain on the northwest and on the south. Normal faulting along the northwestern flank of the Lanyang Plain is complex. Instead of possessing the simple morphology of a simple normal fault, the Hsueshan

Range front displays a complex family of triangular facets that step up slope from the base of the range [*C.-T. Lee et al.*, 1998] (Figure 14). The southern edge of the Lanyang Plain also appears to be controlled by normal faulting. The seaward extension of these two normal fault systems is not very clear, and the lack of high-resolution bathymetry near the coast prohibits resolution of the issue. However, a submarine scarp along the northeastern extension of the northern normal fault system suggests that the northern structure continues for at least another 15 km. The presence of a submarine canyon just offshore Suao, on the other hand, indicates that the southern structure may not extend very far seaward.

The normal faults that bound the Lanyang Plain are generally considered to be the southwestward extension of normal faults bounding the Okinawa Trough. Bathymetry of the Okinawa Trough indicates that the most active opening area in the recent 2 million years is its southern part [*Hsu et al.*, 1996; *Wang et al.*, 1998], adjacent to the Lanyang Plain.

The Lishan fault, which runs along the Lanyang River valley, upstream from the Ilan Plain, is not likely to be an active structure, despite its linear course. This fault is a major bedrock structure in Taiwan [e.g. *Ho*, 1986, 1988; *Yang*, 1986] (Figure 3), and it has a complicated structural history. Geomorphic evidence, however, indicates that the fault is not likely to be active.

Discussion and earthquake scenarios

A principal motive for our investigation of the active tectonics of Taiwan has been to develop a synoptic view of the island's earthquake potential. What we have found is that the island is divisible into eleven discrete active tectonic domains, and that a unique suite of active structures defines each domain. The descriptions of these active structures above provide a basis for developing simple, preliminary characterizations of the predominant seismic sources for each of the eleven domains.

There are many other questions that our investigation of the island's active tectonics has raised, but digging deeply into these issues is outside the scope of this already lengthy paper. Some of the unresolved questions are these: How will the Taiwan orogeny evolve over the next million or so years? Is it, for example, a valid hypothesis that latitude in Taiwan is a surrogate for maturity of the orogen? If so, we can speculate that progressively more southern parts of the outer-arc ridge and volcanic arc of the Philippine Sea plate will continue to dock with the continental margin in the south while the forearc and arc disengage from the continental margin in the north.

Figure 3 shows that the Central Range is not included in any of the domains. Why is there no separate Central Range Domain? This is because we have found no clear geomorphic evidence for active faulting through the high mountains. Many of the active structures of the domains dip toward the Central Range, but we estimate that these structures pass through the brittle-ductile transition where we have drawn the mountain-ward edge of each domain. This may be at odds, however, with recent work that shows minor seismicity continuing well below what we have assumed to be the brittle-ductile transition [e.g., *Wu et al.*, 1997; *Rau and Wu*, 1998; *Kao and Chen*, 2000; *Carena et al.*, 2002]. Farther into and farther beneath the mountains, we assume any major structures behave aseismically. We have not resolved whether these extend through the brittle-ductile transition, or if strain beneath the high mountains occurs by penetrative deformation. We suspect that, however, it is the pervasive ductile crustal thickening that produces the rapid uplift of the Central Range. Any deeper ductile detachment(s) must interact somehow with the presumably steep contact that separates the lithosphere of the continental shelf (i.e., Western Foothills and Hsueshan Range) and that of the forearc ridge (i.e., Central Range).

Why is the active architecture of Taiwan divisible into discrete domains? One possibility is that the geometry of currently active structures is controlled by pre-existing faults. It is well known that some of the currently active structures have re-occupied older structures. For example, the Shanchiao fault, the principal active fault of the Taipei Domain, occupies much of the plane of the inactive Hsinchuang thrust fault. Many inactivated normal faults of the continental margin are now also partially reactivated by active thrust faults of the Hsinchu and Taichung Domains. Perhaps the lengths of the currently active faults are influenced by the lengths of these older faults. Another plausible reason for the discreteness of the domains may have to do with the efficiency of breaking crustal rocks. The fact that fault planes re-rupture is an indication that less energy is expended by the re-rupture of a favorably oriented pre-existing fault plane than by fresh rupture of unfaulted rock. This should be true even in an evolving orogen, in which a pre-existing fault will re-rupture until creation of a new fault becomes more efficient energetically. The discreteness of the faults and their transition zones may be a reflection of this basic principle. It may be only at rare critical junctures in the history of a fault that the fault becomes inactive and that new structures are born.

The transition zone between the Taichung and Miaoli Domains provides a possible example of this. The 1999 mountain-front rupture from about Fengyuan northward lies farther east than an older trace of the Chelungpu fault (Figure 10). The anticlinal welt that ruptured eastward in 1999 from the younger trace of the Chelungpu into the Tachia River also appears to represent a very young feature, perhaps with only a few earlier paleoseismic events. The hook-like map pattern of the new branch of the Chelungpu fault and the anticlinal welt is geometrically very similar to the hook-like pattern of the old Chelungpu and Sanyi faults about 10 km farther north (Figure 10). The old hook may well represent a recently abandoned, more northern end of the Chelungpu fault zone. If so, the northern end of the fault zone has jumped recently about 10 km southward from the northern hook to the southern one. Resolution of this question about the discreteness of the domains will come only with more detailed geochronologic, stratigraphic and geomorphic work.

What seismic events can Taiwan expect in the next century or two? To begin to answer this question, we must know the geometries and slip characteristics of the active faults in each domain. These characteristics are not known well or uniformly for all the domains. Nonetheless, we can estimate major source shapes and locations well enough to give a preliminary notion of the major earthquakes that should be expected. This will be the main focus of the discussion below.

Seismic moment (M_o) is a parameter that we can estimate from structural data:

$$M_o = \mu WLD$$

where μ is the shear modulus, commonly about $3*10^{11}$ dyne/cm^2 in the crust; W is the down-dip width of the rupture; L is the along-strike length of the rupture; and D is the average slip across the rupture plane. Furthermore, these structural parameters are directly related via seismic moment to earthquake moment magnitude (M_w), by another formula:

$$M_w = 2/3 \text{ Log } M_o - 10.73$$

Furthermore, moment magnitude has the following relationship to rupture area (A, in km^2), based upon published regression results [e.g., *Wells and Coppersmith*, 1994]:

$$M_w = 3.98 + 1.02 * \log A, \text{ for strike-slip faults,}$$

$$M_w = 3.93 + 1.02 * \log A, \text{ for normal faults, and,}$$

$$M_w = 4.33 + 0.90 * \log A, \text{ for reverse faults.}$$

Since rupture area equals rupture length (L) times down-dip rupture width (W), we can estimate the magnitudes of future earthquakes in Taiwan's eleven domains from the data we have presented in this paper and figure out a reasonable average slip in a typical earthquake event for a given structure.

In each domain, we have identified the surface manifestations of the one or more predominant structures. Thus, we can estimate the length of future seismic ruptures. This presumes, of course, that like the 1999 Chelungpu rupture, the entire length of the fault is involved, and the rupture does not spill over significantly onto other faults.

Since this is not always the case, our estimates of magnitude using the entire length (L) of a fault will be maximum values for individual faults. We would have overestimated, for example, the size of the earthquakes in the Longitudinal Valley in 1951, since only portions of the fault broke during those events. On the other hand, since ruptures sometimes break across structural complexities [e.g., *Matsuda*, 1974; *Sieh et al.*, 1993; *Eberhart-Phillips et al.*, 2003], using just the length of one major fault can significantly underestimate the magnitude of complex earthquakes. With these caveats in mind, however, we use fault length for rupture length in the calculations below, because it provides a simple starting point for future discussions.

Our estimates of down-dip width (W) derive from estimates of the dips of the faults and the depth of the brittle-ductile transition. For the depth of the brittle-ductile transition, we would use the depth of greatest upper-crustal seismicity, if it were not for the fact that in Taiwan this presents a confusing picture. Numerous deep crustal earthquakes beneath the island, especially in its eastern part, have in fact inspired *Wu et al.* [1997] to propose that the Taiwan orogeny results from lithospheric collision as distinct from thin-skinned tectonics. Therefore, in most cases, we make the simple assumption that the brittle-ductile transition beneath the island is everywhere at a depth of 15 km. The brittle-plastic transition of quartz occurs at approximately 300˚C [e.g., *Kerrich et al.*, 1977; *Tullis and Yund*, 1977], and that of feldspar occurs at approximately 500˚C [e.g., *White*, 1975; *Tullis and Yund*, 1977]. The average geothermal gradient of Taiwan is approximately 30°C/km [e.g., *Huang*, 1990]. Given the fact that most of the rocks in the upper crust of Taiwan are quartz-rich sedimentary rocks, a 15 km brittle-ductile transition is therefore a reasonable and conservative estimation. In fact, few earthquakes occur at a depth greater than 15 km in western Taiwan [e.g., *Carena et al.*, 2002].

Certainly, this estimate is only a first-cut attempt and we have ignored many possible variations in seismogenic depth [e.g., *Scholz*, 2002; *Nazareth and Hauksson*, 2004]. In a few cases we use better information. For example, for the Chelungpu fault, model inversions of co-seismic geodetic displacements and seismograms provide excellent constraints on the depth of the co-seismic rupture plane.

For fault dips we use published structural analyses, where available and credible. Elsewhere, we use conventional dips of 30˚, 60˚ and 90˚ for thrust, normal and strike-slip faults, respectively, with steeper dips for thrust faults if there is a component of slip along strike. Figure 15 displays these interpretations, drawn from a variety of sources. Several are from published sources, but others are our own sketches.

Figure 16 is a map of the major seismic structures that we propose. Table 1 accompanies this graphical representation of the same data. It includes the values of length (L), width (W), average slip (D), as well as other parameters that we have used in estimating the magnitude of earthquake associated with each source. On the map, each source appears as a polygon, with surface traces solid and the surface projections of subsurface edges dashed. For most of the domains, the dashed lines closest to the Central Range represent our estimate of the down-dip limit of seismic rupture, based upon a 15-km depth for the brittle-ductile transition.

The Lutao-Lanyu Domain is dominated by a major fault that crops out along the eastern base of the Huatung Ridge (Figure 16). Based upon published seismic reflection and topographic data, we believe that the Huatung Ridge thrust crops out south of about 22˚20'N but may be blind farther north. We assume a dip of about 30 degrees west for the fault [e.g., *Lundberg et al.*, 1997; *Chang et al.*, 2001; *Malavieille et al.*, 2002]. The resulting moment magnitudes (M_w) would be about 7.6 for the fault (Figure 16). Average slip across the fault would be about 2.4 meters based upon the seismic moment that we have calculated.

The east-dipping fault that we propose beneath the island of Lutao appears to be significantly shorter, perhaps only 40 km long. The length and width of this fault suggest a maximum magnitude of 7.0. The lesser thrust fault that dips southeast beneath the southern part of the Huatung Ridge at about 22˚N (Figure 4) is only about 30 km long, so the largest magnitude we would expect from it is in the high 6s.

The Taitung Domain has two and probably three principal seismic sources (Figure 16). The clearest is the steeply east-dipping Longitudinal Valley fault, which has significant components of both thrust and left-lateral strike-slip motion. If the entire length of the fault in the Longitudinal Valley were to rupture in a single event, the magnitude could well be 7.4 (Table 1). We have also argued for activity of the west-dipping Central Range fault within the Taitung Domain, but we have no reliable estimate of its dip. Its 80-km length and an assumed dip of 45˚ yields a maximum magnitude of 7.2. Evidence for activity of the west-dipping thrust fault that appears to daylight 20 km offshore is sparser still. If this is, indeed, an active, 120-km long structure, we would predict a maximum magnitude of about 7.4. Of these three, only the Longitudinal Valley fault has ruptured historically, in the M7.0 and M6.2 earthquakes of 1951 [*Shyu et al.*, 2005b] and during smaller events in 1995 and 2003 [*Chen and Rau*, 2002; *R.-J. Rau*, unpublished data]. Creep at rapid rates is well known along parts of this fault, but geodetic measurements are too sparse to allow determination of the full extent of the creep, either along strike or down dip. Furthermore, the temporal stability of the current pattern of creep is unknown. More work will be necessary to define better the extent to which creep of the fault reduces the threat of seismic rupture.

Within the Hualien Domain, the Longitudinal Valley fault appears to be the only active structure. Earthquakes produced by this fault in 1951 were magnitude 7.3 and 7.1 and the surface rupture involved only approximately 6% of the total subaerial extent of the fault. The length of the fault within the Hualien Domain yields a hypothetical largest event of M_w 7.2.

The Ryukyu Domain encompasses the seismic Ryukyu subduction zone, the largest seismogenic source of Taiwan. The seismic portion of the subduction interface in the westernmost part of the Ryukyu trench is limited approximately to that portion above a depth of about 35 km [*Kao et al.*, 1998]. Thus, only that ~50-km wide strip between the trench and the Ryukyu Islands is likely to generate great subduction earthquakes. The eastern limit of the interface is hard to specify. At about 123˚E, however, the Gagua Ridge collides with the Ryukyu trench, and creates a major geometric irregularity in the Ryukyu subduction interface [e.g., *Sibuet and Hsu*, 1997; *Schnürle et al.*, 1998] (Figure 1a). The dip angle of the Wadati-Benioff zone changes dramatically across the longitude of the Gagua Ridge, from 65˚ on the west to 50˚ on the east [e.g., *Deschamps et al.*, 2000]. We assume that this geometric break about 150 km east of Taiwan's east coast is a barrier to rupture propagation. This leads to calculation of a magnitude 8.0 as the largest plausible event on the subduction interface near Taiwan. Two large events with magnitudes greater than 8.0 in 1910 and 1920 [*Hsu*, 1980; *Cheng and Yeh*, 1989] most plausibly originated on this strip of the subduction interface.

The normal fault system along the coast between the Longitudinal Valley and the Lanyang Plain is about 50 km long. We therefore calculate a maximum magnitude of 6.9 and an average slip of about 1.2 meters for this zone (Table 1 and Figure 16).

In the Kaoping Domain three active structures appear to dominate (Figures 15 and 16). One of these is the Chaochou fault zone. As discussed previously, this fault may extend southeastward to connect with the strike-slip Hengchun fault. Alternatively, it may also extend southward along a submarine canyon to about the latitude of the southern tip of Taiwan (Figure 8). In either scenario, this possibly high-angle fault has a total length of about 120 km, and is capable of producing an earthquake of about M_w 7.3 (Table 1). Rupture of only the onland portion of the Chaochou fault could also produce a M_w 7.2 earthquake. Another major structure in the Kaoping Domain is the strike-slip fault along the western margin of the Pingtung Plain. Its length yields a maximum magnitude of 6.9. The other structure is the deformation front, which is likely to be a reverse fault that runs all the way to the Manila trench in the south. Between the latitudes of Tainan and Kaohsiung, there is no topographic evidence for the existence of this reverse fault. But to the south, numerous folds and minor faults on the seafloor are likely to be the result of irregularities in the underlying deformation front and secondary structures above it. This huge reverse fault system has a length of at least 200 km in Figure 3, and might produce an earthquake event of at least M_w 7.7.

We have discussed four main constraints on the nature of the principal active structures in the Chiayi Domain. These are the young deformation of the coastal plain and the Chiayi Hills, abundant small to moderate earthquakes between the coast and the Western Foothills, structural interpretations based upon well data and surface outcrops, and interpretations of geodetic data. Several secondary features, such as the Hsiaomei anticline and the minor thrust faults in the Chiayi Hills, the duplexes and backthrusts of structural models, and the source faults of the 1906, 1946, 1999 and other earthquakes complicate the neotectonic picture. The historical fault ruptures demonstrate that many secondary structures exist within the domain and that some are capable of producing earthquakes in the upper 6s. The 1906 and 1946 events represent earthquakes produced by faults in the transition zones with neighboring domains. The M6.4 earthquake in October 1999 may represent events within crystalline bedrock of the continental shelf, well below the principal detachment that *Suppe* [1976, 1980b] proposed to exist within the Neogene shelf strata.

Acknowledging these complications, let us focus here on the potential for rupture of the principal structure within the Chiayi Domain. If we adopt the interpretations of *Hsu et al.* [2003] regarding the large horizontal gradient in GPS vectors, we can plot a rapidly creeping detachment about as shown on Figure 15. In their model, the creeping detachment dips about 15˚ eastward and extends up-dip as far as the eastern edge of our definition of the Chiayi Domain. A reasonable initial interpretation would be that a locked detachment extends westward from this edge to a position beneath the western edge of deformation, near the coast. This is our basis for proposing the source depicted beneath the Chiayi Domain in Figures 15 and 16. Judging from its width and length, the size of the resultant earthquake would be about M_w 7.5, with an average slip of approximately 2.3 meters (Table 1). A M6.5 earthquake in 1930 and a M7.2 earthquake in 1941 [*Hsu*, 1980; *Cheng and Yeh*, 1989] could have been produced by partial rupture of this structure, although rupture of two secondary structures within the domain could also have produced these earthquakes.

The Chelungpu and the Changhua faults are the two major seismogenic structures of the Taichung Domain (Figures 15 and 16). Rupture of the entire Chelungpu fault and the accommodation structure on its north end in 1999 resulted in the M_w 7.6 Chi-Chi earthquake. The Changhua fault has a length similar to that of the Chelungpu, but the dip of the fault may be shallower than the Chelungpu fault in its deeper part (Figure 15). This suggests that rupture of the entire Changhua fault could produce an earthquake of even greater magnitude than the Chi-Chi event (Table 1).

As we have seen, the major active fault or faults of the Miaoli Domain are not as well defined as those in the Taichung Domain. The largest historical earthquake produced within the domain was the M7.1 event of 1935. Two disparate surface ruptures are associated with this earthquake – a right-lateral accommodation structure and a bedding-plane fault on the eastern limb of a tightly folded syncline. No modern inversion of the seismograms of this earthquake has been attempted, so we do not know if these two ruptures were accompanied by rupture of the underlying detachment. However, the size of the earthquake indicates it might have involved rupture of more than just the two known secondary structures (Table 1).

The active folds and faults of the Miaoli Domain are probably subordinate to a major active detachment that underlies the domain (Figures 15 and 16). In calculating the length of the detachment, we assume that it extends southward beneath the transition zone with the Taichung Domain. We do not know whether or not to include the faults of the Hsinchu Domain, since these could be the northern wrap-around of the Miaoli Domain. If we terminate the detachment at the border with the Hsinchu Domain, we calculate a maximum magnitude of 7.3 for earthquakes produced by the detachment (Table 1). If, however, we extend the detachment through the entire the Hsinchu Domain, we derive a maximum magnitude of 7.5. By comparison, separate rupture of the Shihtan backthrust yields only a M_w 6.1 earthquake (Figure 16).

The Touhuanping fault in the transition zone between the Hsinchu and Miaoli Domains is a major strike-slip fault with a length up to 25 km. Rupture of this major accommodation structure is capable of producing an earthquake with a maximum magnitude of 6.6 (Table 1).

The Hsinchu Domain encompasses the densely populated regions of Hsinchu and Taoyuan. The principal emergent seismic sources include those of the Taoyuan-Hukou Tableland and of the Hsinchu-Hsincheng system (Figure 16). If they were to rupture together, the thrust faults and right-lateral faults of the Taoyuan-Hukou Tableland are large enough to produce a complex earthquake of about M_w 7.1 (Table 1). Separate failure of the largest of these structures, the Hukou fault, would produce about a M_w 6.9 event. Similarly, if all the thrust and strike-slip faults of the Hsinchu-Hsincheng system failed in unison, an earthquake of about M_w 6.8 would result. But if just the Hsinchu or Hsincheng fault failed separately, events of about M_w 6.5 and 6.6 would result.

The two major active structures in the Ilan Domain, the normal fault zones along the northwestern and southern flanks of the Lanyang Plain, are the bounding structures of the disengagement of the continental and forearc lithospheres of the Hsueshan and Central Ranges. These structures have on-land lengths of 75 and 25 km, but it is not clear how far seaward they extend. The northern structure may extend at least 15 km offshore, and the southern one is likely to end near the coastline. The resultant lengths for these two normal fault systems then yield maximum magnitudes of 7.2 and 6.6, respectively (Table 1 and Figure 16). The thick and rapidly accumulating sediments of the Lanyang Plain may well obscure other active normal faults between the two bounding faults within the back-arc basin. These would be additional potential sources of future earthquakes.

A seismic scenario for the Taipei Domain is one of the easiest to estimate, because there is only one principal active fault, the Shanchiao (Figures 15 and 16). The threat posed by this active normal fault may be the greatest of any in Taiwan, because the fault dips beneath the metropolitan region of Taipei, the capital and most populous city of the island. If we assume that a single rupture of the Shanchiao fault would extend only along the western edge of the Taipei basin, the resultant earthquake would have a magnitude of about M_w 6.5, with an average fault slip of about 0.7 meter (Table 1). If, however, we postulate that a single rupture could continue from the edge of the basin over the volcanic edifice to the north, the rupture length becomes about 45 km, and we calculate a M_w 6.9, with about 1.1 meters of dip slip. Paleoseismic investigations may be able to resolve the rupture lengths of past earthquakes and provide some insight into which of these scenarios is more probable. One recent analysis, in fact, shows that two possible ruptures between 8 and 10 ka may have involved as much as 3 to 4 meters of slip [*Huang et al.*, 2005]. Such large slips imply even longer ruptures than we have proposed.

Vertical offsets of one to three meters are common along active normal faults with lengths as great as the Shanchiao fault. Offsets of this size would have particularly serious consequences for Taipei, because large portions of the Taipei basin are less than 3 meters above sea level. The submergence event of AD 1694 may thus be related to rupture of the fault.

Now that we have presented plausible seismic sources for all of Taiwan's neotectonic domains, we are tempted to calculate the frequency with which large earthquakes from these sources might visit each domain. This could be done using modern geodetic rates of horizontal shortening to estimate the average amount of time necessary to accumulate the strain relieved by each scenario event. These calculations would be simplest for the domains dominated by single faults, such as the Chiayi and Taipei Domains. For example, elastic strain accumulation equal to that relieved by 2.3

meters of offset on the Chiayi detachment (our scenario event) would accumulate in only about 65 years, if the detachment is the only structure to release the strain. However, for the Taipei Domain, the rate of strain accumulation is so low that the errors in GPS vectors are too large to allow such a calculation. In complex domains, such as Kaoping, Lutao-Lanyu, Hsinchu and Ilan, the long-term partitioning of deformation across the faults is so poorly known that calculations of average recurrence intervals using modern geodetically determined strain rates would not be very meaningful.

In some cases, it would be more reliable to divide the cumulative slip on the principal faults over the past million or so years by the amount of slip that we anticipate in future events. For the Shanchiao fault in the Taipei Domain, for example, this yields an average interval of approximately 500 to 600 years. In other cases, short paleoseismic records are beginning to provide direct evidence of recurrence intervals. For example, *Streig et al.* [2005] have shown that the previous rupture of the central part of the Chelungpu fault was similar to the 1999 rupture in slip magnitude and occurred about 640-740 years ago. However, in most domains, geochronologic, stratigraphic and structural controls on late Quaternary strata are still too poor to constrain recurrence intervals meaningfully.

Another complication in estimating average return periods for large earthquakes is the degree to which the major faults are creeping in the upper crust. Some, such as the Chihshang fault in the Taitung Domain, are known to be creeping rapidly at the surface [*Angelier et al.*, 1997; *Lee et al.*, 2001] and probably at depth [*Chen and Rau*, 2002]. Complicating this is the fact that the rupture of 1951 earthquake extended into this creeping sector [*Hsu*, 1962; *Shyu et al.*, 2005b]. More detailed narrow-aperture geodetic experiments similar to those of *Angelier et al.* [1997] and *Lee et al.* [2001] and broad-aperture experiments as well are needed to resolve the importance of creep in diminishing the rate of production of large earthquakes in Taiwan.

In conclusion, then, the current state of structural, stratigraphic, rheological and geodetic knowledge precludes us from offering meaningful calculations of average return times for seismic rupture of the large faults within each domain. Instead, we suggest that rigorous, multi-disciplinary programs be established to constrain average and actual recurrence intervals.

Conclusions

Using a 40-meter-resolution DEM, augmented by structural, geodetic and seismologic data, we have prepared a neotectonic map and cross-sections of Taiwan. The active structures we have identified suggest that the Taiwan orogen is due to a tandem suturing and tandem disengagement of a volcanic arc and a continental sliver to and from the Eurasian continental margin. Moreover, the island of Taiwan is divided naturally into distinct neotectonic domains, each with distinct principal structures. Four domains are present along the eastern suture, and seven domains comprise the western suture. These domains and their principal structures provide a basis for understanding future earthquakes around Taiwan. Using simple regression models, we have also proposed possible earthquake scenarios for each of the domains. These results should assist the many ongoing geodetic, geophysical, paleoseismic and other attempts to understand future seismic hazard of the island.

Acknowledgments

We are grateful for valuable discussions with J.-P. Avouac, O. Beyssac, Y.-C. Chan, W.-C. Chi, H.-T. Chu, M.-L. Hsieh, J.-C. Hu, J.-C. Lee, C.-H. Lo, C.-Y. Lu, Y. Ota, C. Rubin, M. Simons, Q. Sung, L.S. Teng, B. Wernicke, and S.-B. Yu. Also, we have benefited from stimulating discussions with students of two field classes in Taiwan and a neotectonic seminar at National Taiwan University. The comments and suggestions of reviewers I. Manighetti and R.S. Yeats greatly helped us improve this manuscript. Our mapping would have been impossible had C.-T. Lee not made us aware that high-quality digital topography of the island existed. J. Giberson, manager of the Caltech's GIS laboratory, helped with the technical aspects of mapping. Our project in Taiwan was initially supported by private funds of Caltech's Division of Geological and Planetary Sciences and later by NSF grant EAR-0208505. This research was also supported in part by the Gordon and Betty Moore Foundation. This is Caltech Tectonic Observatory Contribution #3.

References

Angelier, J., H.-T. Chu, and J.-C. Lee (1997), Shear concentration in a collision zone: kinematics of the Chihshang Fault as revealed by outcrop-scale quantification of active faulting, Longitudinal Valley, eastern Taiwan, *Tectonophysics*, *274*, 117-143.

Barrier, E., and J. Angelier (1986), Active collision in eastern Taiwan: the Coastal Range, *Mem. Geol. Soc. China*, *7*, 135-159.

Biq, C. (1965), The East Taiwan Rift, *Pet. Geol. Taiwan*, *4*, 93-106.

Biq, C. (1972), Dual-trench structure in the Taiwan-Luzon region, *Proc. Geol. Soc. China*, *15*, 65-75.

Biq, C. (1992), Another Coastal Range on Taiwan (in Chinese with English summary), *Ti-Chih*, *12*, 1-12.

Bonilla, M. G. (1975), A review of recently active faults in Taiwan, *Open File Rep. 75-41*, 58pp., U. S. Geol. Surv., Menlo Park, Calif.

Bonilla, M. G. (1977), Summary of Quaternary faulting and elevation changes in Taiwan, *Mem. Geol. Soc. China*, *2*, 43-55.

Carena, S., J. Suppe, and H. Kao (2001), Imaging the main detachment under Taiwan: implications for the critical-taper mechanics and large-scale topography, *EOS*, *Trans.*, *Am. Geophys. Uni.*, *82*(47), Fall Meet. Suppl., Abstract T32A-0863.

Carena, S., J. Suppe, and H. Kao (2002), Active detachment of Taiwan illuminated by small earthquakes and its control of first-order topography, *Geology*, *30*, 935-938.

Central Geologic Survey (1999a), Map of surface ruptures along the Chelungpu fault during the Chi-Chi earthquake, Taiwan, scale 1:25,000, Cent. Geol. Surv., Ministry Econ. Affairs, Taipei, Taiwan.

Central Geologic Survey (1999b), Report of the geological survey of the 1999 Chi-Chi earthquake (in Chinese), 314pp., Cent. Geol. Surv., Ministry Econ. Affairs, Taipei, Taiwan.

Chan, Y.-C., J.-C. Lee, C.-Y. Lu, and H.-T. Chu (2001), Transtensional tectonics along a major north-south trending fault in the active convergent Taiwan mountain belt, *EOS*, *Trans.*, *Am. Geophys. Uni.*, *82*(47), Fall Meet. Suppl., Abstract T32A-0880.

Chan, Y. C., J. C. Lee, C. Y. Lu, J. C. Hu, H. T. Chu, C. S. Hou, R. J. Rau, and K. E. Ching (2002), Neotectonic and structural characteristics along the Chaochou fault system in SW Taiwan: implications for tectonic escape during oblique plate convergence, *EOS*, *Trans.*, *Am. Geophys. Uni.*, *83*(47), Fall Meet. Suppl., Abstract T62D-12.

Chang, C. P., J. Angelier, C. Y. Huang, and C. S. Liu (2001), Structural evolution and significance of a mélange in a collision belt: the Lichi Mélange and the Taiwan arc-continent collision, *Geol. Mag., 138*, 633-651.

Chang, H.-C., C.-W. Lin, M.-M. Chen, and S.-T. Lu (1998), *An Introduction to the Active Faults of Taiwan, Explanatory Text of the Active Fault Map of Taiwan* (in Chinese with English abstract), *Spec. Pub. Cent. Geol. Surv.*, *10*, 103pp., Cent. Geol. Surv., Ministry Econ. Affairs, Taipei, Taiwan.

Chang, J.-C., T.-T. Shih, S.-M. Shen, and C.-L. Chang (1992), A geomorphological study of river terrace in northern Huatung Longitudinal Valley (in Chinese with English abstract), *Geogr. Res., 18*, 1-51.

Chang, J.-C., K.-H. Teng, and M.-C. Liu (1998), A geomorphological study on river terraces in Miaoli Hills (in Chinese with English abstract), *Geogr. Res.*, *29*, 97-112.

Chang, L.-S., M. Chow, and P.-Y. Chen (1947), The Tainan earthquake of December 5, 1946 (in Chinese with English summary), *Bull. Geol. Surv. Taiwan*, *1*, 11-18 (Chinese), and 17-20 (English).

Chang, S. S. L. (1974), Subsurface geologic study of the Miaoli area, Taiwan, *Pet. Geol. Taiwan*, *11*, 1-25.

Chemenda, A. I., R. K. Yang, C.-H. Hsieh, and A. L. Groholsky (1997), Evolutionary model for the Taiwan collision based on physical modelling, *Tectonophysics*, *274*, 253-274.

Chemenda, A., S. Lallemand, and A. Bokun (2000), Strain partitioning and interplate friction in oblique subduction zones: Constraints provided by experimental modeling, *J. Geophys. Res.*, *105*, 5,567-5,581.

Chen, C.-Y. (1974), Verification of the north-northeastward movement of the Coastal Range, eastern Taiwan, by re-triangulation (in Chinese with English abstract), *Bull. Geol. Surv. Taiwan*, *24*, 119-123.

Chen, H.-H., and R.-J. Rau (2002), Earthquake locations and style of faulting in an active arc-continent plate boundary: the Chihshang fault of eastern Taiwan, *EOS, Trans., Am. Geophys. Uni.*, *83*(47), Fall Meet. Suppl., Abstract T61B-1277.

Chen, J.-S. (1978), A comparative study of the refraction and reflection seismic data obtained on the Changhua plain to the Peikang Shelf, Taiwan, *Pet. Geol. Taiwan*, *15*, 199-217.

Chen, M.-P., Y.-T. Shieh, and C.-S. Shyr (1988), Seafloor physiography and surface sediments off southeastern Taiwan, *Acta Geol. Taiwanica*, *26*, 333-353.

Chen, R.-F. (1999), Geomorphic index study of active structures in Chiayi-Tainan area, southwestern Taiwan (in Chinese with English abstract), M.S. thesis, 146pp., Natl.

Cheng Kung Univ., Tainan, Taiwan.

Chen, W.-S., Y.-M. Cheng, and C.-Y. Huang (1985), Geology of the Hengchun Peninsula, southern Taiwan (in Chinese with English abstract), *Ti-Chih*, *6*(2), 47-74.

Chen, W.-S., Y.-G. Chen, T.-K. Liu, N.-W. Huang, C.-C. Lin, S.-H. Sung, and K.-J. Lee (2000), Characteristics of the Chi-Chi earthquake ruptures (in Chinese with English abstract), *Spec. Pub. Cent. Geol. Surv.*, *12*, 139-154.

Chen, Y.-G. (1993), Sea-level change and neotectonics in southern part of Taiwan region since Late Pleistocene (in Chinese), Ph.D. thesis, 158pp., Natl. Taiwan Univ., Taipei, Taiwan.

Chen, Y.-G., and T.-K. Liu (1992), Vertical crustal movement of a tectonic uplifting volcanic island – Lutao, *J. Geol. Soc. China*, *35*, 231-246.

Chen, Y.-G., W.-S. Chen, J.-C. Lee, Y.-H. Lee, C.-T. Lee, H.-C. Chang, and C.-H. Lo (2001), Surface rupture of 1999 Chi-Chi earthquake yields insights on active tectonics of central Taiwan, *Bull. Seismol. Soc. Am.*, *91*, 977-985.

Chen, Y.-G., W.-S. Chen, Y. Wang, P.-W. Lo, T.-K. Liu, and J.-C. Lee (2002), Geomorphic evidence for prior earthquakes: Lessons from the 1999 Chichi earthquake in central Taiwan, *Geology*, *30*, 171-174.

Cheng, S. N., and Y. T. Yeh (1989), *Catalog of the Earthquakes in Taiwan from 1604 to 1988* (in Chinese), 255pp., Inst. Earth Sci., Acad. Sinica, Taipei, Taiwan.

Cheng, S.-N., Y. T. Yeh, and M.-S. Yu (1996), The 1951 Taitung earthquake in Taiwan, *J. Geol. Soc. China*, *39*, 267-285.

Chinese Petroleum Corporation (1994), The geologic map of Miaoli, scale 1:100,000, *No. 3*, Taiwan Pet. Exploration Div., Chinese Pet. Corp., Miaoli, Taiwan.

Deschamps, A., P. Monié, S. Lallemand, S.-K. Hsu, and K. Y. Yeh (2000), Evidence for Early Cretaceous oceanic crust trapped in the Philippine Sea Plate, *Earth Planet. Sci. Lett.*, *179*, 503-516.

Eberhart-Phillips, D., et al. (2003), The 2002 Denali fault earthquake, Alaska: a large magnitude, slip-partitioned event, *Science*, *300*, 1,113-1,118.

Elishewitz, B. (1963), A new interpretation of the structure of the Miaoli area in the light of the décollement tectonics of northwest Taiwan, *Pet. Geol. Taiwan*, *2*, 21-45.

Font, Y., C.-S. Liu, P. Schnurle, and S. Lallemand (2001), Constraints on backstop geometry of the southwest Ryukyu subduction based on reflection seismic data, *Tectonophysics*, *333*, 135-158.

Fruneau, B., E. Pathier, D. Raymond, B. Deffontaines, C. T. Lee, H. T. Wang, J. Angelier, J. P. Rudant, and C. P. Chang (2001), Uplift of Tainan Tableland (SW Taiwan) revealed by SAR interferometry, *Geophys. Res. Lett.*, *28*, 3,071-3,074.

Gilbert, G. K. (1890), *Lake Bonneville, U. S. Geol. Surv. Monograph I.*, 438pp., U. S. Geol. Surv., Washington, D. C.

Hanai, S. (1930), Active faults in the Toen Hill, Formosa (in Japanese), *Geogr. Rev. Japan*, *6*(7), 778-789.

Hayasaka, I. (1935), On the earthquake of April, 21, 1935 in Sintiku and Taityû Prefectures (in Japanese), *Taiwan Tigaku Kizi*, *6*(6), 58-78.

Ho, C. S. (1986), A synthesis of the geologic evolution of Taiwan, *Tectonophysics*, *125*, 1-16.

Ho, C. S. (1988), *An Introduction to the Geology of Taiwan, Explanatory Text of the Geologic Map of Taiwan*, 2nd ed., 192pp., Cent. Geol. Surv., Ministry Econ. Affairs, Taipei, Taiwan.

Hou, C.-S., L.-Y. Fei, and T.-C. Lai (1998), GPS investigation in the Pingtung Plain (in Chinese with English abstract), *Proceedings of the Symposium on Groundwater and Hydrogeology of the Pingtung Plain*, 239-251, Taipei, Taiwan.

Hovius, N., C. P. Stark, H.-T. Chu, and J.-C. Lin (2000), Supply and removal of sediment in a landslide-dominated mountain belt: Central Range, Taiwan, *J. Geol.*, *108*, 73-89.

Hsiao, P. T. (1971), Seismic study of the area between the coastal plain and the foothills, Yunlin, Taiwan, *Pet. Geol. Taiwan*, *8*, 249-263.

Hsiao, P. T. (1974), Subsurface geologic study of the Hsinying coastal plain area, Taiwan, *Pet. Geol. Taiwan*, *11*, 27-39.

Hsieh, C.-H., Y.-F. Chang, and R.-H. Sun (1992), Seismic investigate Hsin-Chuan fault on the west of Taipei Basin (in Chinese with English abstract), *Ti-Chih*, *12*(1), 13-26.

Hsu, M.-T. (1980), *Earthquake Catalogues in Taiwan (from 1644 to 1979)* (in Chinese), 77pp., Natl. Taiwan Univ., Taipei, Taiwan.

Hsu, S.-K., J.-C. Sibuet, S. Monti, C.-T. Shyu, and C.-S. Liu (1996), Transition between the Okinawa Trough backarc extension and the Taiwan collision: new insights on the southernmost Ryukyu subduction zone, *Mar. Geophys. Res.*, *18*, 163-187.

Hsu, T. L. (1955), Earthquakes in Taiwan (in Chinese), *Quart. J. Bank Taiwan*, *7*(2), 148-164.

Hsu, T. L. (1962), Recent faulting in the Longitudinal Valley of eastern Taiwan, *Mem. Geol. Soc. China*, *1*, 95-102.

Hsu, T. L., and H. C. Chang (1979), Quaternary faulting in Taiwan, *Mem. Geol. Soc. China*, *3*, 155-165.

Hsu, W.-L. (2001), Detecting the Changhua fault and its neighboring structures (in Chinese with English abstract), M.S. thesis, 94pp., Natl. Cent. Univ., Chungli, Taiwan.

Hsu, Y.-J., M. Simons, S.-B. Yu, L.-C. Kuo, and H.-Y. Chen (2003), A two-dimensional dislocation model for interseismic deformation of the Taiwan mountain belt, *Earth Planet. Sci. Lett.*, *211*, 287-294.

Hu, J.-C., J. Angelier, C. Homberg, J.-C. Lee, and H.-T. Chu (2001), Three-dimensional modeling of the behavior of the oblique convergent boundary of southeast Taiwan: friction and strain partitioning, *Tectonophysics*, *333*, 261-276.

Huang, C.-Y., C.-T. Shyu, S. B. Lin, T.-Q. Lee, and D. D. Sheu (1992), Marine geology in the arc-continent collision zone off southeastern Taiwan: Implications for Late Neogene evolution of the Coastal Range, *Mar. Geol.*, *107*, 183-212.

Huang, C.-Y., W.-Y. Wu, C.-P. Chang, S. Tsao, P. B. Yuan, C.-W. Lin, and K.-Y. Xia (1997), Tectonic evolution of accretionary prism in the arc-continent collision terrane of Taiwan, *Tectonophysics*, *281*, 31-51.

Huang, C.-Y., P. B. Yuan, C.-W. Lin, T. K. Wang, and C.-P. Chang (2000), Geodynamic processes of Taiwan arc-continent collision and comparison with analogs in Timor, Papua New Guinea, Urals and Corsica, *Tectonophysics*, *325*, 1-21.

Huang, G.-T. (1996), Preliminary study on the tectonic geomorphology in the southwestern Foothills, Taiwan (in Chinese), M.S. thesis, 114pp., Natl. Cent. Univ., Chungli, Taiwan.

Huang, L. S. (1990), Preliminary study on the subsurface temperature and geothermal gradients of the late Cenozoic basin in western Taiwan (in Chinese with English abstract), *Bull. Cent. Geol. Surv.*, *6*, 117-144.

Huang, M.-T., W.-L. Wang, K.-L. Pan, and T. P. Yen (1985), Photogeologic study of active fault II: The Meishan surface fault (in Chinese with English abstract), *Hazard Mitigation Res. Rep. 73-29*, 42pp., Natl. Sci. Council, Taipei, Taiwan.

Huang, S.-Y., C. M. Rubin, Y.-G. Chen, and H.-C. Liu (2005), Prehistoric earthquakes along the Shanchiao Fault, Taipei Basin, Northern Taiwan, *J. Asian Earth Sci.*, submitted.

Hung, J.-H. (1996), Structure of Western Foothills and crustal deformation in southwestern Taiwan (in Chinese with English abstract), *Program with Abstracts, 1996 Ann. Meet. Geol. Soc. China*, 436-440, Taipei, Taiwan.

Hung, J.-H., and D. V. Wiltschko (1993), Structure and kinematics of arcuate thrust faults in the Miaoli-Cholan area of western Taiwan, *Pet. Geol. Taiwan*, *28*, 59-96.

Hung, J.-H., D. V. Wiltschko, H.-C. Lin, J. B. Hickman, P. Fang, and Y. Bock (1999), Structure and motion of the southwestern Taiwan Fold and Thrust Belt, *Terr. Atmos. Oceanic Sci.*, *10*, 543-568.

Ji, C., D. V. Helmberger, T.-R. A. Song, K.-F. Ma, and D. J. Wald (2001), Slip distribution and tectonic implication of the 1999 Chi-Chi, Taiwan, Earthquake, *Geophys. Res. Lett.*, *28*, 4,379-4,382.

Kao, H., and W.-P. Chen (2000), The Chi-Chi earthquake sequence: active, out-of-sequence thrust faulting in Taiwan, *Science*, *288*, 2,346-2,349.

Kao, H., and R.-J. Rau (1999), Detailed structures of the subducted Philippine Sea plate beneath northeast Taiwan: A new type of double seismic zone, *J. Geophys. Res.*, *104*, 1,015-1,033.

Kao, H., S.-s. J. Shen, and K.-F. Ma (1998), Transition from oblique subduction to collision: Earthquakes in the southernmost Ryukyu arc-Taiwan region, *J. Geophys. Res.*, *103*, 7,211-7,229.

Kao, H., G.-C. Huang, and C.-S. Liu (2000), Transition from oblique subduction to collision in the northern Luzon arc-Taiwan region: Constraints from bathymetry and seismic observations, *J. Geophys. Res.*, *105*, 3,059-3,079.

Kelson, K. I., K.-H. Kang, W. D. Page, C.-T. Lee, and L. S. Cluff (2001), Representative styles of deformation along the Chelungpu fault from the 1999 Chi-Chi (Taiwan) earthquake: Geomorphic characteristics and responses of man-made structures, *Bull. Seismol. Soc. Am.*, *91*, 930-952.

Kerrich, R., R. D. Beckinsale, and J. J. Durham (1977), The transition between deformation regimes dominated by intercrystalline diffusion and intracrystalline creep evaluated by oxygen isotope thermometry, *Tectonophysics*, *38*, 241-257.

Kizaki, K. (1986), Geology and tectonic framework of the Ryukyu Islands, *Mem. Geol. Soc. China*, *7*, 1-14.

Ku, C.-C. (1963), Photogeologic study of terraces in northwestern Taiwan, *Proc. Geol. Soc. China*, *6*, 51-60.

Lacombe, O., F. Mouthereau, B. Deffontaines, J. Angelier, H. T. Chu, and C. T. Lee (1999), Geometry and Quaternary kinematics of fold-and-thrust units of southwestern Taiwan, *Tectonics*, *18*, 1,198-1,223.

Lacombe, O., F. Mouthereau, J. Angelier, and B. Deffontaines (2001), Structural, geodetic and seismological evidence for tectonic escape in SW Taiwan, *Tectonophysics*, *333*, 323-345.

Lallemand, S., and C.-S. Liu (1998), Geodynamic implications of present-day kinematics in the southern Ryukyus, *J. Geol. Soc. China*, *41*, 551-564.

Lallemand, S. E., C.-S. Liu, and ACT cruise scientific team (1997), Swath bathymetry reveals active arc-continent collision near Taiwan, *EOS, Trans., Am. Geophys. Uni.*, *78*(17), 173-175.

Lallemand, S., C.-S. Liu, S. Domingues, P. Schnürle, J. Malavieille, and the ACT Scientific Crew (1999), Trench-parallel stretching and folding of forearc basins and lateral migration of the accretionary wedge in the southern Ryukyus: A case of strain partition caused by oblique convergence, *Tectonics*, *18*, 231-247.

Lee, C.-T., C.-T. Cheng, C.-W. Liaw, and Y.-B. Chang (1998), Active fault map of Taiwan, Inst. Applied Geology, Natl. Cent. Univ., Chungli, Taiwan.

Lee, J.-C., H.-T. Chu, C.-Y. Lu, B. Deffontaines, O. Lacombe, F. Mouthereau, J. Angelier, and B. Delcaillau (1997), Structural characteristics of the Changhua thrust zone, western Taiwan (in Chinese), *Program and Expanded Abstracts, 1997 Ann. Meet. Geol. Soc. China*, 313-314, Tainan, Taiwan.

Lee, J.-C., J. Angelier, H.-T. Chu, S.-B. Yu, and J.-C. Hu (1998), Plate-boundary strain partitioning along the sinistral collision suture of the Philippine and Eurasian plates: Analysis of geodetic data and geological observation in southeastern Taiwan, *Tectonics*, *17*, 859-871.

Lee, J.-C., J. Angelier, H.-T. Chu, J.-C. Hu, and F.-S. Jeng (2001), Continuous monitoring of an active fault in a plate suture zone: a creepmeter study of the Chihshang Fault, eastern Taiwan, *Tectonophysics*, *333*, 219-240.

Lee, J.-C., H.-T. Chu, J. Angelier, Y.-C. Chan, J.-C. Hu, C.-Y. Lu, and R.-J. Rau (2002), Geometry and structure of northern surface ruptures of the 1999 Mw = 7.6 Chi-Chi Taiwan earthquake: influence from inherited fold belt structures, *J. Struct. Geol.*, *24*, 173-192.

Lee, Y.-H., W.-Y. Wu, T.-S. Shih, S.-T. Lu, M.-L. Hsieh, and H.-C. Chang (2000), Deformation characteristics of surface ruptures of the Chi-Chi earthquake, east of the Pifeng Bridge (in Chinese with English abstract), *Spec. Pub. Cent. Geol. Surv.*, *12*, 19-40.

Lin, C.-C. (1957), *Geomorphology of Taiwan* (in Chinese), 424pp., Taiwan Prov. Literature Comm., Taipei, Taiwan.

Lin, C.-W., H.-C. Chang, S.-T. Lu, T.-S. Shih, and W.-J. Huang (2000a), *An Introduction to the Active Faults of Taiwan, 2nd ed., Explanatory Text of the Active Fault Map of Taiwan* (in Chinese with English abstract), *Spec. Pub. Cent. Geol. Surv.*, *13*, 122pp., Taipei, Taiwan.

Lin, C.-W., S.-T. Lu, W.-J. Huang, T.-S. Shih, and H.-C. Chang (2000b), The Chi-Chi earthquake fault and structural analysis of the area south of Choshuihsi, central Taiwan (in Chinese with English abstract), *Spec. Pub. Cent. Geol. Surv.*, *12*, 89-111.

Lin, H.-Y. (1998), Depositional system of the Maanshan Formation, Hengchun Peninsula (in Chinese), M.S. thesis, 74pp., Natl. Sun Yat-sen Univ., Kaohsiung, Taiwan.

Liu, C.-C., and S.-B. Yu (1990), Vertical crustal movements in eastern Taiwan and their tectonic implications, *Tectonophysics*, *183*, 111-119.

Liu, C.-S., I. L. Huang, and L. S. Teng (1997), Structural features off southwestern Taiwan, *Mar. Geol.*, *137*, 305-319.

Liu, C.-S., S.-Y. Liu, S. E. Lallemand, N. Lundberg, and D. L. Reed (1998), Digital elevation model offshore Taiwan and its tectonic implications, *Terr. Atmos. Oceanic Sci.*, *9*, 705-738.

Lu, S., T.-H. Lai, and C.-J. Chiang (1998), Long-term subsidence rates of the Pingtung Plain (in Chinese with English abstract), *Proceedings of the Symposium on Groundwater and Hydrogeology of the Pingtung Plain*, 153-163, Taipei, Taiwan.

Lundberg, N., D. L. Reed, C.-S. Liu, and J. Lieske, Jr. (1992), Structural controls on orogenic sedimentation, submarine Taiwan collision, *Acta Geol. Taiwanica*, *30*, 131-140.

Lundberg, N., D. L. Reed, C.-S. Liu, and J. Lieske, Jr. (1997), Forearc-basin closure and arc accretion in the submarine suture zone south of Taiwan, *Tectonophysics*, *274*, 5-23.

Ma, K.-F., T.-R. A. Song, S.-J. Lee, and H.-I. Wu (2000), Spatial slip distribution of the September 20, 1999, Chi-Chi, Taiwan, earthquake (Mw7.6)—Inverted from teleseismic data, *Geophys. Res. Lett.*, *27*, 3,417-3,420.

Ma, K.-F., J. Mori, S.-J. Lee, and S. B. Yu (2001), Spatial and temporal distribution of slip for the 1999 Chi-Chi, Taiwan, earthquake, *Bull. Seismol. Soc. Am.*, *91*, 1,069-1,087.

Malavieille, J., S. E. Lallemand, S. Dominguez, A. Deschamps, C.-Y. Lu, C.-S. Liu, P. Schnürle, and the ACT Scientific Crew (2002), Arc-continent collision in Taiwan: new marine observations and tectonic evolution, *Geol. Soc. Am. Spec. Paper*, *358*, 187-211.

Matsuda, T. (1974), Surface faults associated with Nobi (Mino-Owari) earthquake of 1891, Japan (in Japanese with English abstract), *Spec. Bull. Earthquake Res. Inst., Univ. Tokyo*, *13*, 85-126.

Namson, J. (1981), Structure of the Western Foothills belt, Miaoli-Hsinchu area, Taiwan: (I) Southern part, *Pet. Geol. Taiwan*, *18*, 31-51.

Namson, J. (1983), Structure of the Western Foothills belt, Miaoli-Hsinchu area, Taiwan: (II) Central part, *Pet. Geol. Taiwan*, *19*, 51-76.

Namson, J. (1984), Structure of the Western Foothills belt, Miaoli-Hsinchu area, Taiwan: (III) Northern part, *Pet. Geol. Taiwan*, *20*, 35-52.

Nazareth, J. J., and E. Hauksson (2004), The seismogenic thickness of the southern California crust, *Bull. Seismol. Soc. Am.*, *94*, 940-960.

Omori, F. (1907), Preliminary note on the Formosa earthquake of March 17, 1906, *Bull. Imp. Earthquake Invest. Comm.*, *1*(2), 53-69.

Ota, Y., J. B. H. Shyu, Y.-G. Chen, and M.-L. Hsieh (2002), Deformation and age of fluvial terraces south of the Choushui River, central Taiwan, and their tectonic implications, *Western Pacific Earth Sci.*, *2*, 251-260.

Otuka, Y. (1936), The earthquake of central Taiwan (Formosa), April 21, 1935, and earthquake faults (in Japanese with English résumé), *Bull. Earthquake Res. Inst., Tokyo Imp. Univ., Suppl. 3*, 22-74.

Pan, K.-L., W.-N. Wang, K.-H. Hu, and T.-P. Yen (1983), Photogeologic investigations of the earthquake fault of 1935, central Taiwan (in Chinese), *Hazard Mitigation Res. Rep. 72-20*, 48pp., Natl. Sci. Council, Taipei, Taiwan.

Pan, Y. S., and C.-C. Hu (1972), An analysis on the sea bottom topography of the offshore area west of Hsinchu and Miaoli, Taiwan, *Pet. Geol. Taiwan*, *10*, 339-349.

Rau, R.-J., and F. T. Wu (1998), Active tectonics of Taiwan orogeny from focal mechanisms of small-to-moderate-sized earthquakes, *Terr. Atmos. Oceanic Sci.*, *9*, 755-778.

Reed, D. L., N. Lundberg, C.-S. Liu, and B.-Y. Kuo (1992), Structural relations along the margins of the offshore Taiwan accretionary wedge: implications for accretion and crustal kinematics, *Acta Geol. Taiwanica*, *30*, 105-122.

Schnürle, P., C.-S. Liu, S. E. Lallemand, and D. L. Reed (1998), Structural insight into the south Ryukyu margin: effects of the subducting Gagua Ridge, *Tectonophysics*, *288*, 237-250.

Scholz, C. H. (2002), *The Mechanics of Earthquakes and Faulting*, 2nd ed., 471pp., Cambridge University Press, Cambridge, UK.

Shieh, Y.-T. (2000), The paleogeography of the ancient Taipei lakebed in the K'anghsi Period (in Chinese with English abstract), *J. Geogr. Sci.*, *27*, 85-95.

Shih, R.-C., P.-H. Chen, H.-Y. Yen, and C.-H. Lin (2000), Geophysical investigations on active faults in the central part of Taiwan and Taitung area (in Chinese), *2000 Ann. Rep., Geophysical Investigation Projects on Active Faults*, 126pp., Cent. Geol. Surv., Ministry Econ. Affairs, Taipei, Taiwan.

Shih, R.-C., P.-H. Chen, M.-T. Lu, W.-S. Chen (2002), Earthquake geology investigation and the construction of the active faults database (in Chinese), *2002 Ann. Rep., Geophysical Investigation Projects on Active Faults*, 166pp., Cent. Geol. Surv., Ministry Econ. Affairs, Taipei, Taiwan.

Shih, T.-T., and G.-S. Yang (1985), The active faults and geomorphic surfaces of Pakua Tableland in Taiwan (in Chinese with English abstract), *Geogr. Res.*, *11*, 173-186.

Shih, T.-T., J.-C. Chang, and G.-S. Yang (1983), The active faults and geomorphic surfaces of Houli Tableland in Taiwan (in Chinese), *Bull. Geogr. Soc. China*, *11*, 46-55.

Shih, T.-T., K.-H. Teng, J.-C. Chang, C.-D. Shih, G.-S. Yang, and M.-Y. Hsu (1984a), A geomorphological study of active fault in western and southern Taiwan (in Chinese with English abstract), *Geogr. Res.*, *10*, 49-94.

Shih, T.-T., K.-H. Teng, and G.-S. Yang (1984b), The active faults and geomorphic surfaces of Tatu Tableland in Taiwan (in Chinese), *Bull. Geogr. Soc. China*, *12*, 9-21.

Shih, T.-T., K.-H. Teng, J.-C. Chang, and G.-S. Yang (1985), The active faults and geomorphic surfaces of Hengchun area in Taiwan (in Chinese with English abstract), *Geogr. Education*, *11*, 1-14.

Shih, T.-T., K.-H. Teng, J.-C. Chang, C.-D. Shih, and G.-S. Yang (1986), A geomorphological study of active fault in Taiwan (in Chinese with English abstract), *Geogr. Res.*, *12*, 1-44.

Shyu, J. B. H. (1999), The sedimentary environment of southern Pingdong Plain since the Last Glacial (in Chinese with English abstract), M.S. thesis, 212pp., Natl. Taiwan Univ., Taipei, Taiwan.

Shyu, J. B. H., K. Sieh, L.-H. Chung, Y.-G. Chen, and Y. Wang (2002), The active tectonics of eastern Taiwan—new insights from the two geomorphic tablelands ("the Feet") in the Longitudinal Valley, *EOS, Trans., Am. Geophys. Uni.*, *83*(47), Fall Meet. Suppl., Abstract T61B-1278.

Shyu, J. B. H., K. Sieh, and Y.-G. Chen (2005a), Tandem suturing and disarticulation of the Taiwan orogen revealed by its neotectonic elements, *Earth Planet. Sci. Lett.*, submitted.

Shyu, J. B. H., L.-H. Chung, Y.-G. Chen, J.-C. Lee, and K. Sieh (2005b), Re-evaluation of the surface ruptures of the November 1951 earthquake series in eastern Taiwan, and its neotectonic implications, *J. Asian Earth Sci.*, submitted.

Sibuet, J.-C., and S.-K. Hsu (1997), Geodynamics of the Taiwan arc-arc collision, *Tectonophysics*, *274*, 221-251.

Sieh, K., et al. (1993), Near field investigations of the Landers earthquake sequence, April to July 1992, *Science*, *260*, 171-176.

Stach, L. W. (1958), Subsurface exploration and geology of the coastal plain region of western Taiwan, *Proc. Geol. Soc. China*, *1*, 55-96.

Streig, A. R., C. M. Rubin, W.-S. Chen, Y.-G. Chen, L.-S. Lee, S.-T. Lu, S. Thompson, and S.-Y. Huang (2005), Evidence for prehistoric coseismic folding along the Tsaotun segment of the Chelungpu fault near Nan-Tou, Taiwan: Seismic hazard along active fold scarps, *J. Geophys. Res.*, in press.

Sun, R.-H. (1990), The seismic survey on the subsurface structures in the western edge (Wuku-Taishan) area of Taipei Basin (in Chinese), M.S. thesis, 61pp., Natl. Cent. Univ., Chungli, Taiwan.

Sun, S. C. (1970), Photogeologic study of the Tainan-Hsinying coastal plain, Taiwan, *Pet. Geol. Taiwan*, *7*, 133-144.

Sun, S. C. (1971), Photogeologic study of the Hsinying-Chiayi coastal plain, Taiwan, *Pet. Geol. Taiwan*, *8*, 65-75.

Sun, S. C. (1972), Photogeologic study of the Peikang-Choshuichi coastal plain, Taiwan, *Pet. Geol. Taiwan*, *10*, 187-199.

Sung, Q.-C., and Y. Wang (1985), Petrofacies of Miocene sediments in the Hengchun Peninsula and its tectonic implication, *Proc. Geol. Soc. China*, *28*, 23-44.

Sung, Q., and Y. Wang (1986), Sedimentary environments of the Miocene sediments in the Hengchun Peninsula and their tectonic implication, *Mem. Geol. Soc. China*, *7*, 325-340.

Sunlin, Y.-M. (1982), A geomorphological study on active faults on the Taoyuan Tablelands (in Chinese), M.S. thesis, 53pp., Natl. Taiwan Normal Univ., Taipei, Taiwan.

Suppe, J. (1976), Décollement folding in southwestern Taiwan, *Pet. Geol. Taiwan*, *13*, 25-35.

Suppe, J. (1980a), A retrodeformable cross section of northern Taiwan, *Proc. Geol. Soc. China*, *23*, 46-55.

Suppe, J. (1980b), Imbricated structure of western foothills belt, southcentral Taiwan, *Pet. Geol. Taiwan*, *17*, 1-16.

Suppe, J. (1981), Mechanics of mountain building and metamorphism in Taiwan, *Mem. Geol. Soc. China*, *4*, 67-89.

Suppe, J. (1984), Kinematics of arc-continent collision, flipping of subduction, and back-arc spreading near Taiwan, *Mem. Geol. Soc. China*, *6*, 21-33.

Suppe, J. (1987), The active Taiwan mountain belt, in *Anatomy of Mountain Chains*, edited by J. P. Schaer, and J. Rodgers, pp. 277-293, Princeton Univ. Press, Princeton, N.J.

Suppe, J., and J. Namson (1979), Fault-bend origin of frontal folds of the western Taiwan fold-and-thrust belt, *Pet. Geol. Taiwan*, *16*, 1-18.

Tan, K. (1939), Geological consideration on the Taihoku Basin (in Japanese with English abstract), *Jubilee Pub. Commemoration Prof. H. Yabe, M. I. A., 60th Birthday*, *1*, 371-380.

Tan, L. P. (1977), Pleistocene eastward bending of the Taiwan arc, *Mem. Geol. Soc. China*, *2*, 77-83.

Tang, C. H. (1963), Geology and oil potentialities of the Hukou anticline, Hsinchu, *Pet. Geol. Taiwan*, *2*, 241-252.

Teng, L. S. (1987), Stratigraphic records of the late Cenozoic Penglai orogeny of Taiwan, *Acta Geol. Taiwanica*, *25*, 205-224.

Teng, L. S. (1990), Late Cenozoic arc-continent collision in Taiwan, *Tectonophysics*, *183*, 57-76.

Teng, L. S. (1996), Extensional collapse of the northern Taiwan mountain belt, *Geology*, *24*, 949-952.

Teng, L. S., C. T. Lee, Y. B. Tsai, L.-Y. Hsiao (2000), Slab breakoff as a mechanism for flipping of subduction polarity in Taiwan, *Geology*, *28*, 155-158.

Teng, L. S., C. T. Lee, C.-H. Peng, W.-F. Chen, and C.-J. Chu (2001), Origin and geological evolution of the Taipei Basin, northern Taiwan, *Western Pacific Earth Sci.*, *1*, 115-142.

Tong, L.-T., and C.-H. Yang (1999), Geophysical survey and stratigraphic correlations of the Chianan Plain (in Chinese), *Cent. Geol. Surv. Rep. 88-017*, 122pp., Cent. Geol. Surv., Ministry Econ. Affairs, Taipei, Taiwan.

Tullis, J., and R. A. Yund (1977), Experimental deformation of dry Westerly granite, *J. Geophys. Res.*, *82*, 5,705-5,718.

Wang, C., M.-L. Yung, C.-S. Lee, and C.-P. Chou (1998), Morphology and seismicity distribution of the Okinawa Trough: western extension to the island of Taiwan (in Chinese), *Program and Abstracts, 1998 Ann. Meet. Geol. Soc. China*, 115, Chungli, Taiwan.

Wang, C.-Y., G.-P. Chen, and D.-T. Jong (1994), The detection of active faults on Taiwan using shallow reflection seismics, *Terr. Atmos. Oceanic Sci.*, *5*, 277-293.

Wang, P. C. M. (1964), Reflection seismic survey conducted on the Hukou-Yangmei structure, Taiwan, *Pet. Geol. Taiwan*, *3*, 185-191.

Wang, P. C. M. (1967), Subsurface geology and oil possibilities of the Taoyuan-Miaoli offshore region, Taiwan, *Pet. Geol. Taiwan*, *5*, 81-98.

Wang, Y. (2003), Morphotectonics in Taoyuan-Hsinchu area, northwestern Taiwan (in Chinese with English abstract), M.S. thesis, 105pp., Natl. Taiwan Univ., Taipei, Taiwan.

Wang-Lee, C. M., Y. M. Cheng, and Y. Wang (1978), Geology of the Taipei Basin (in Chinese), *Taiwan Mining Industry*, *30*(4), 350-380.

Wells, D. L., and K. J. Coppersmith (1994), New empirical relationships among magnitude, rupture length, rupture width, rupture area, and surface displacement, *Bull. Seismol. Soc. Am.*, *84*, 974-1,002.

White, S. (1975), Tectonic deformation and recrystallisation of oligoclase, *Contrib. Mineral. Petrol.*, *50*, 287-304.

Wu, F.-T. (1965), Subsurface geology of the Hsinchuang structure in the Taipei Basin, *Pet. Geol. Taiwan*, *4*, 271-282.

Wu, F. T. (1978), Recent tectonics of Taiwan, *J. Phys. Earth*, *26*, Suppl., S265-S299.

Wu, F. T., R.-J. Rau, and D. Salzberg (1997), Taiwan orogeny: thin-skinned or lithospheric collision?, *Tectonophysics*, *274*, 191-220.

Yang, G.-S. (1986), A geomorphological study of active faults in Taiwan – especially on the relation between active faults and geomorphic surfaces (in Chinese), Ph.D. thesis, 178pp., Chinese Culture Univ., Taipei, Taiwan.

Yang, K.-M., J.-C. Wu, J. S. Wickham, H.-H. Ting, J.-B. Wang, and W.-R. Chi (1996), Transverse structures in Hsinchu and Miaoli areas: structural mode and evolution in foothills belt, northwestern Taiwan, *Pet. Geol. Taiwan*, *30*, 111-150.

Yang, K.-M., H.-H. Ting, J.-C. Wu, and W.-R. Chi (1997), Geological model for complex structures and its implications for hydrocarbon exploration in northwestern Taiwan, *Pet. Geol. Taiwan*, *31*, 1-42.

Yang, K.-M., M.-G. Yeh, J.-C. Wu, and Z.-F. Sun (2000), Geometry, characteristics and evolution of Changhua fault and its associated structures (in Chinese with English abstract), *Program and Abstracts, 2000 Ann. Meet. Geol. Soc. China*, 103-105, Taipei, Taiwan.

Yang, S.-H. (1999), Determination of the fault locations using surface movement – examples from the Hualien area (in Chinese), M.S. thesis, 92pp., Natl. Cent. Univ., Chungli, Taiwan.

Yang, Y.-C. (1953), Earthquakes in Hualien in the latest 41 years (in Chinese), *Hualien Literatures*, *1*, 67-71.

Yeats, R. S., K. Sieh, and C. R. Allen (1997), *The Geology of Earthquakes*, 568pp., Oxford Univ. Press, New York.

Yeh, M.-G., W.-S. Chen, and W.-C. Shyr (1999), Seismic study of the Pliocene to Pleistocene Series in the southwest plain, Taiwan (in Chinese with English abstract), *Pet. Geol. Taiwan*, *33*, 199-215.

Yu, M.-S. (1997), Active faults in the Taitung Longitudinal Valley (in Chinese), Ph.D. thesis, 141pp., Natl. Taiwan Univ., Taipei, Taiwan.

Yu, S.-B., and H.-Y. Chen (1998), Strain accumulation in southwestern Taiwan, *Terr. Atmos. Oceanic Sci.*, *9*, 31-50.

Yu, S.-B., and L.-C. Kuo (2001), Present-day crustal motion along the Longitudinal Valley Fault, eastern Taiwan, *Tectonophysics*, *333*, 199-217.

Yu, S.-B., and C.-C. Liu (1989), Fault creep on the central segment of the Longitudinal Valley fault, eastern Taiwan, *Proc. Geol. Soc. China*, *32*, 209-231.

Yu, S.-B., H.-Y. Chen, and L.-C. Kuo (1997), Velocity field of GPS stations in the Taiwan area, *Tectonophysics*, *274*, 41-59.

Yu, S.-B., L.-C. Kuo, R. S. Punongbayan, and E. G. Ramos (1999), GPS observation of crustal deformation in the Taiwan-Luzon region, *Geophys. Res. Lett.*, *26*, 923-926.

Figure Captions

Figure 1. A neotectonic snapshot of Taiwan and adjacent regions. (a) Taiwan is currently experiencing a double suturing: In the south, the Luzon volcanic arc is colliding with the Hengchun forearc ridge, which is, in turn, colliding with the Eurasian continental margin. In the north, both sutures are unstitching. Their disengagement is forming both the Okinawa Trough and the forearc basins of the Ryukyu arc. Thus, in the course of passing through the island, the roles of the volcanic arc and forearc ridge flip along with the flipping of the polarity of subduction. The three gray strips represent the three lithospheric pieces of Taiwan's tandem suturing and disarticulation: the Eurasian continental margin, the continental sliver, and the Luzon arc. Black arrows indicate the suturing and disarticulation. This concept is discussed in detail in *Shyu et al.* [2005a]. Current velocity vector of the Philippine Sea plate relative to the Eurasian plate adapted from *Yu et al.* [1997, 1999]. Current velocity vector of the Ryukyu arc adapted from *Lallemand and Liu* [1998]. Black dashed lines are the northern and western limits of the Wadati-Benioff zone of the two subducting systems, taken from the seismicity database of the Central Weather Bureau, Taiwan. DF: deformation front; LCS: Lishan-Chaochou suture; LVS: Longitudinal Valley suture; WF: Western Foothills; CeR: Central Range; CoR: Coastal Range; HP: Hengchun Peninsula. (b) Major tectonic elements around Taiwan. Active structures identified in this study are shown in red. Major inactive faults that form the boundaries of tectonic elements are shown in black: 1: Chiuchih fault; 2: Lishan fault; 3: Laonung fault; 4: Chukou fault. Selected GPS vectors relative to the stable Eurasian continental shelf adapted from *Yu et al.* [1997]. A: Western Foothills; B: Hsueshan Range; C: Central Range and Hengchun Peninsula; D: Coastal Range; E: westernmost Ryukyu arc; F: Yaeyama forearc ridge; G: northernmost Luzon arc; H: western Taiwan coastal plains; I: Lanyang Plain; J: Pingtung Plain; K: Longitudinal Valley; L: submarine Hengchun Ridge; M: Ryukyu forearc basins.

Figure 2. Two examples showing the geomorphic evidence for active structures visible in the 40-m DEM. Figures of similar resolution for other part of Taiwan are available as electronic data supplements. Locations of the two are shown in Figure 1(b). (a) Along a southern segment of the Chelungpu fault, topographic features not only readily predict the locations of the 1999 major rupture (marked by black arrows), but also show a minor, secondary fault rupture (marked by a red arrow) and a monoclinal surface rupture on the hanging wall of the fault (marked by blue arrows). (b) Near the southern end of the Longitudinal Valley, eastern Taiwan, geomorphic features clearly show a thrust fault along the western edge of the Peinanshan (marked by black arrows). The same fault becomes a series of anticlinal folds north of the Luyeh River (marked by red arrows), and eventually steps eastward to the western base of the river terraces east of Rueiyuan (marked by blue arrows). Fluvial surfaces in northern part of the Peinanshan clearly warped into an anticline (in red) and a syncline (in blue).

Figure 3. Map of major active faults and folds of Taiwan (in red) shows that the two sutures are producing separate western and eastern neotectonic belts. Each collision belt matures and then decays progressively from south to north. This occurs in discrete steps, manifested as seven distinct neotectonic domains along the western belt and four along the eastern. A distinctive assemblage of active structures defines each domain. For example, two principal structures dominate the Taichung Domain. Rupture in 1999 of one of these, the Chelungpu fault, caused the disastrous Chi-Chi earthquake. The Lishan fault (dashed black line) is the suture between forearc ridge and continental margin. Bold light green and pink lines are boundaries of domains.

Figure 4. Active-tectonic map of the Lutao-Lanyu Domain. The Hengchun Peninsula, the Southern Longitudinal Trough, the Huatung Ridge, the Taitung Trough, and the Lutao

and Lanyu volcanic islands are the major geomorphic elements of this domain. The Huatung Ridge is an anticline, produced by slip on a major west-dipping thrust fault. A backthrust crops out in the south along its western base. West of Lutao, an east-dipping thrust fault may be responsible for the fast uplift of the island. The irregular polygon that surrounds the active structures in this and following figures defines the perimeter of the domain.

Figure 5. Active-tectonic map of the Taitung Domain. The east-dipping, oblique-slipping Longitudinal Valley fault along the eastern edge of the Longitudinal Valley and the west-dipping Central Range fault along its western edge are the two major structures. The Longitudinal Valley fault partitions into dip-slip and strike-slip strands near "The Foot," just north of Taitung. The Central Range fault may be blind south of Fuli. Minor, discontinuous left-lateral faults occur near Yuli and east of the Wuhe Tableland.

Figure 6. Active-tectonic map of the Hualien Domain. The Longitudinal Valley fault is the only major active structure in this domain. This fault commonly partitions into separate thrust and left-lateral strands. The faults around Hualien City and in the sea farther northeast are the northward extension of the Longitudinal Valley fault.

Figure 7. Active-tectonic map of the western part of the Ryukyu Domain. The Ryukyu trench is the major element of this domain. Numerous folds are present in its hanging wall. Its western margin includes major right-lateral faults and a complex of normal faults around the Hoping basin, a triangular-shaped graben.

Figure 8. Active-tectonic map of the Kaoping Domain. Offshore, complexities of the Manila subduction interface are producing numerous active folds. Onland, the

left-lateral reverse Chaochou fault separates the Central Range and the Pingtung Plain. The west side of the Pingtung Plain is approximately coincident with another left-lateral fault. Deformation within and west of the Western Foothills includes a complex of numerous short folds and right-lateral faults, which facilitate southwestward extrusion.

Figure 9. Active-tectonic map of the Chiayi Domain. Minor reverse faults and anticlines in the Chiayi Hills and incised streams across the Chianan Coastal Plain betray the presence of a blind thrust fault beneath the region. Geomorphic evidence shows that the Chukou fault, a major bedrock geologic structure in this area, is no longer active.

Figure 10. Active-tectonic map of the Taichung Domain. The Chelungpu fault ruptured along almost the entire length of the domain during the 1999 Chi-Chi earthquake. The Changhua fault is the other major structure. The Taichung Basin is a piggyback basin between these two major thrust faults.

Figure 11. Active-tectonic map of the Miaoli Domain. Two major anticline-syncline pairs indicate that the major active thrust fault of the Miaoli Domain is blind. The Shihtan fault, which ruptured during the 1935 earthquake, is a minor bedding-plane backthrust within the eastern limb of the Chuhuangkeng anticline. The right-lateral Tuntzuchiao fault, which also ruptured during the 1935 event, is an accommodation structure between the Miaoli and Taichung Domains.

Figure 12. Active-tectonic map of the Hsinchu Domain. Two groups of active structures comprise this domain. On the Taoyuan-Hukou Tableland is a complex of reverse faults, folds, and a discontinuous right-lateral fault. South of the Touchien River is a group of active reverse and right-lateral strike-slip faults.

Figure 13. Active-tectonic map of the Taipei Domain. The Taipei Basin is a half-graben, formed by slip in the late Quaternary Period on the Shanchiao normal fault. The fault also extends northeastward and offsets the edifice of the Tatun volcanic edifice. The sudden appearance of a lake in the Taipei Basin in 1694 may have resulted from a large rupture of the Shanchiao fault.

Figure 14. Active-tectonic map of the on-land part of the Ilan Domain. Two major bounding normal faults facilitate the incipient opening of the Okinawa Trough across the Lanyang Plain. Other faults within the domain are poorly known, because of rapid sedimentation rate and lack of high-resolution bathymetry. Focal mechanism and other parameters of the May 15^{th}, 2002, earthquake adapted from the BATS database.

Figure 15. Simple cross-sections proposed for each of the eleven tectonic domains. Each crude, unbalanced cross-section provides tentative geometries of the major active faults, based upon geomorphic, geodetic, structural and seismic data. Red: active structures; black: inactive structures.

Figure 16. Proposed major sources for future large earthquakes in and around Taiwan. Bold red lines are proposed future ruptures, and the white patches are rupture planes projected to the surface. Here we have selected only a few representative scenarios from Table 1 to show in this figure. Earthquake magnitude of each scenario is predicted value from our calculation.

Table 1. Proposed major seismic structures of Taiwan. In this table, we include rupture length (L), width (W), and average slip (D), as well as other perimeters used in estimating the magnitude of earthquakes associated with each source.

Fault name	Fault type*	L (km)	Fault dip (degree)	Down-dip limit (km)	W (km)**	A (km^2)#	M_w##	M_o (10^{25} dyne-cm)+	D (m)++
Lutao-Lanyu Domain									
Huatung Ridge fault	R	140	30	15	30.00	4200.00	7.59	302.96	2.40
SW Taitung fault	R	40	45	15	21.21	848.53	6.97	34.97	1.37
West Lutao fault	R	40	45	15	21.21	848.53	6.97	34.97	1.37
West Huatung Ridge fault	R	30	45	15	21.21	636.40	6.85	23.72	1.24
Taitung Domain									
Longitudinal Valley fault, total	R/SS	160	60	15	17.32	2771.28	7.43	172.83	2.08
Longitudinal Valley fault, Taitung Domain only	R/SS	96	60	15	17.32	1662.77	7.23	86.72	1.74
Central Range fault, total	R	80	45	15	21.21	1697.06	7.24	89.14	1.75
Central Range fault, emerged part only	R	40	45	15	21.21	848.53	6.97	34.97	1.37
Taitung offshore fault	R	120	45	15	21.21	2545.58	7.40	154.10	2.02
Hualien Domain									
Longitudinal Valley fault, Hualien Domain only	SS	90	60	15	17.32	1558.85	7.24	89.12	1.91
Ryukyu Domain									
Ryukyu trench	R	~180	30	35	70.00	12600.00	8.02	1335.06	3.53
The major right-lateral accommodation structure	SS	50	90	15	15.00	750.00	6.91	29.10	1.29

Nanao normal fault system	N	50	60	15	17.32	866.03	6.93	30.51	1.17
Kaoping Domain									
Chaochou fault connecting Hengchun fault	SS/R	120	75	15	15.53	1863.50	7.32	117.11	2.09
Chaochou fault connecting the offshore fault	R/SS	120	75	15	15.53	1863.50	7.27	101.15	1.81
Onland Chaochou fault only	SS/R	75	75	15	15.53	1164.69	7.11	57.06	1.63
West Pingtung Plain fault (Kaoping River fault)	SS	50	90	15	15.00	750.00	6.91	29.10	1.29
The deformation front	R	>200	30	15	30.00	>6000.00	>7.73	>490.34	>2.72
Chiayi Domain									
Main detachment	R	60	15	15	57.96	3477.33	7.52	234.79	2.25
Meishan fault	SS	15	90	15	15.00	225.00	6.38	4.61	0.68
Hsinhua fault	SS	12	90	15	15.00	180.00	6.28	3.28	0.61
Taichung Domain									
Chelungpu fault	R	90	15	12	46.36	4172.80	7.59	300.32	2.40
Changhua fault	R	85	10	12	69.11	5874.35	7.72	476.54	2.70
Miaoli Domain									
Shihtan fault	R	20	75	5	5.18	103.53	6.14	2.04	0.66
Tuntzuchiao fault	SS	20	90	12	12.00	240.00	6.41	5.09	0.71

Shihtan and Tuntzuchiao faults[$]	Complex	--	--	--	--	343.53	6.51	7.13	0.69
Main detachment, only in Miaoli Domain	R	60	30	15	30.00	1800.00	7.26	96.52	1.79
Main detachment, extended to Hsinchu Domain	R	110	30	15	30.00	3300.00	7.50	218.77	2.21
Touhuanping fault	SS	25	90	15	15.00	375.00	6.61	10.08	0.90
Hsinchu Domain									
The northern fault on the Taoyuan-Hukou Tablelands	R	20	30	5	10.00	200.00	6.40	4.97	0.83
The southern fault on the tablelands (Hukou fault)	R	25	30	15	30.00	750.00	6.92	29.60	1.32
The major strike-slip fault on the tablelands	SS	30	90	15	15.00	450.00	6.69	13.32	0.99
Fault system on the tablelands, total[$]	Complex	--	--	--	--	1400.00	7.06	47.89	1.14
Hsinchu fault	R	12	45	15	21.21	254.56	6.50	6.88	0.90
Hsincheng fault	R	10	30	15	30.00	300.00	6.56	8.59	0.95
Other accommodation structures	SS	10	90	15	15.00	150.00	6.20	2.48	0.55
The southern system total[$]	Complex	--	--	--	--	704.56	6.77	17.96	0.85

Ilan Domain									
The northern Ilan fault system	N	90	60	15	17.32	1558.85	7.19	74.99	1.60
The southern Ilan fault system	N	25	60	15	17.32	433.01	6.62	10.56	0.81
Taipei Domain									
Shanchiao fault, only in the west of Taipei Basin	N	20	60	15	17.32	346.41	6.52	7.51	0.72
Shanchiao fault, extended to Chinshan	N	45	60	15	17.32	779.42	6.88	25.97	1.11

*R: reverse fault; SS: strike-slip fault; N: normal fault.

**W equals to down-dip limit divided by the sine value of fault dip.

#A equals to L times W.

##The moment magnitudes were calculated using the following equations: for reverse faults, $M_w = 4.33 + 0.90 * \log A$; for strike-slip faults, $M_w = 3.98 + 1.02 * \log A$; for normal faults, $M_w = 3.93 + 1.02 * \log A$ [*Wells and Coppersmith*, 1994].

+The seismic moments were calculated using the following equation: $M_w = 2/3 \operatorname{Log} M_o - 10.73$.

++The average displacement per event was calculated using the equation $M_o = \mu AD$, where μ equals $3*10^{11}$ dyne/cm^2.

$For complex events resulted from ruptures of multiple faults, the calculations are as followed: first, calculate the seismic moment by adding up the moments of each fault; second, calculate the moment magnitude using the seismic moment calculated above; then, calculate the average displacement using the seismic moment and the sum of the rupture areas.

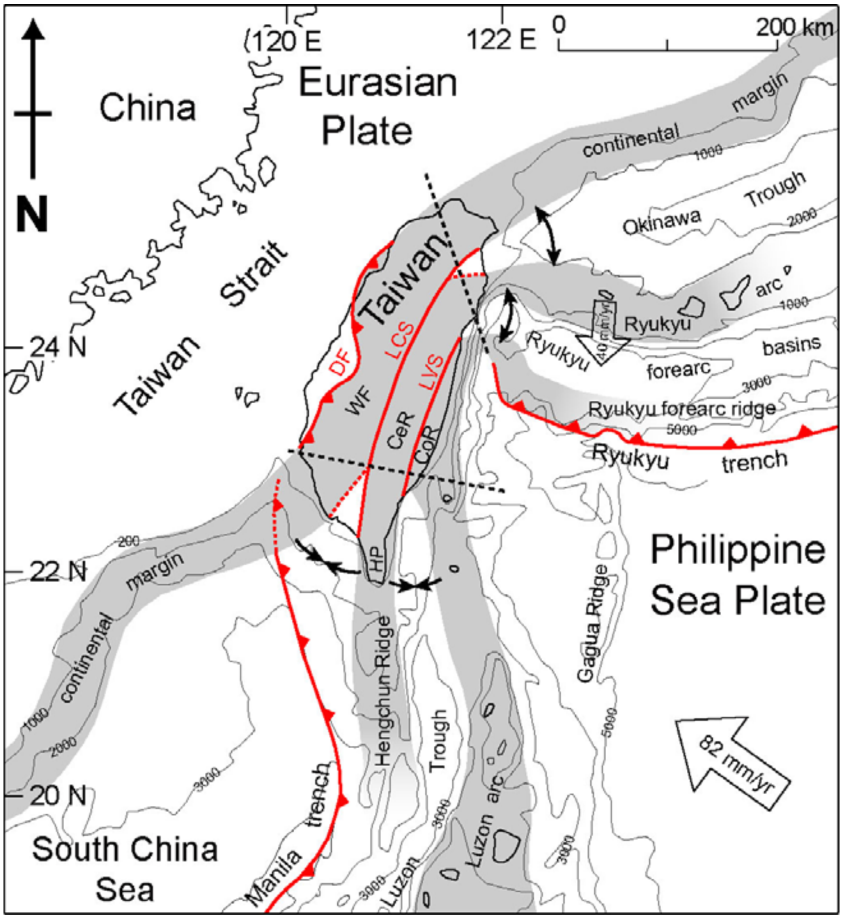
120 E
122 E
0
200 km
N
China
Eurasian Plate
Taiwan Strait
Taiwan
continental margin
Okinawa Trough
Ryukyu arc
Ryukyu forearc basins
Ryukyu forearc ridge
Ryukyu trench
DF
LCS
LVS
WF
CeR
CoR
HP
24 N
22 N
20 N
Philippine Sea Plate
Gagua Ridge
Hengchun Ridge
Trough
Luzon arc
Luzon
82 mm/yr
South China Sea
Manila trench

Figure 1a

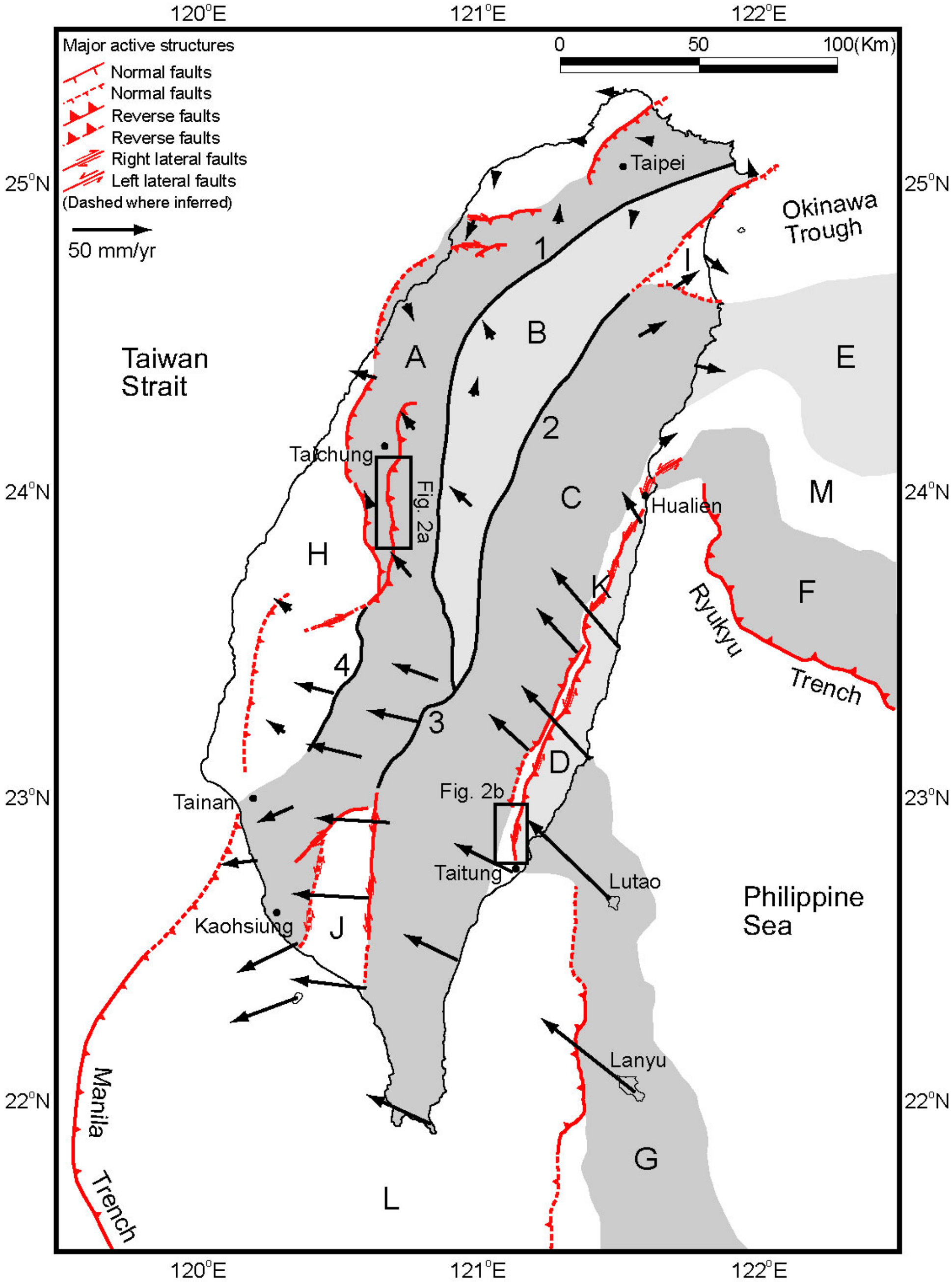
120°E
121°E
122°E
Major active structures
Normal faults
Normal faults
Reverse faults
Reverse faults
Right lateral faults
Left lateral faults
(Dashed where inferred)
50 mm/yr
0
50
100(Km)
25°N
24°N
23°N
22°N
Taipei
Okinawa Trough
Taiwan Strait
Taichung
Fig. 2a
Hualien
Ryukyu Trench
Tainan
Fig. 2b
Taitung
Lutao
Kaohsiung
Philippine Sea
Lanyu
Manila Trench
A
B
C
D
E
F
G
H
I
J
K
L
M
1
2
3
4

Figure 1b

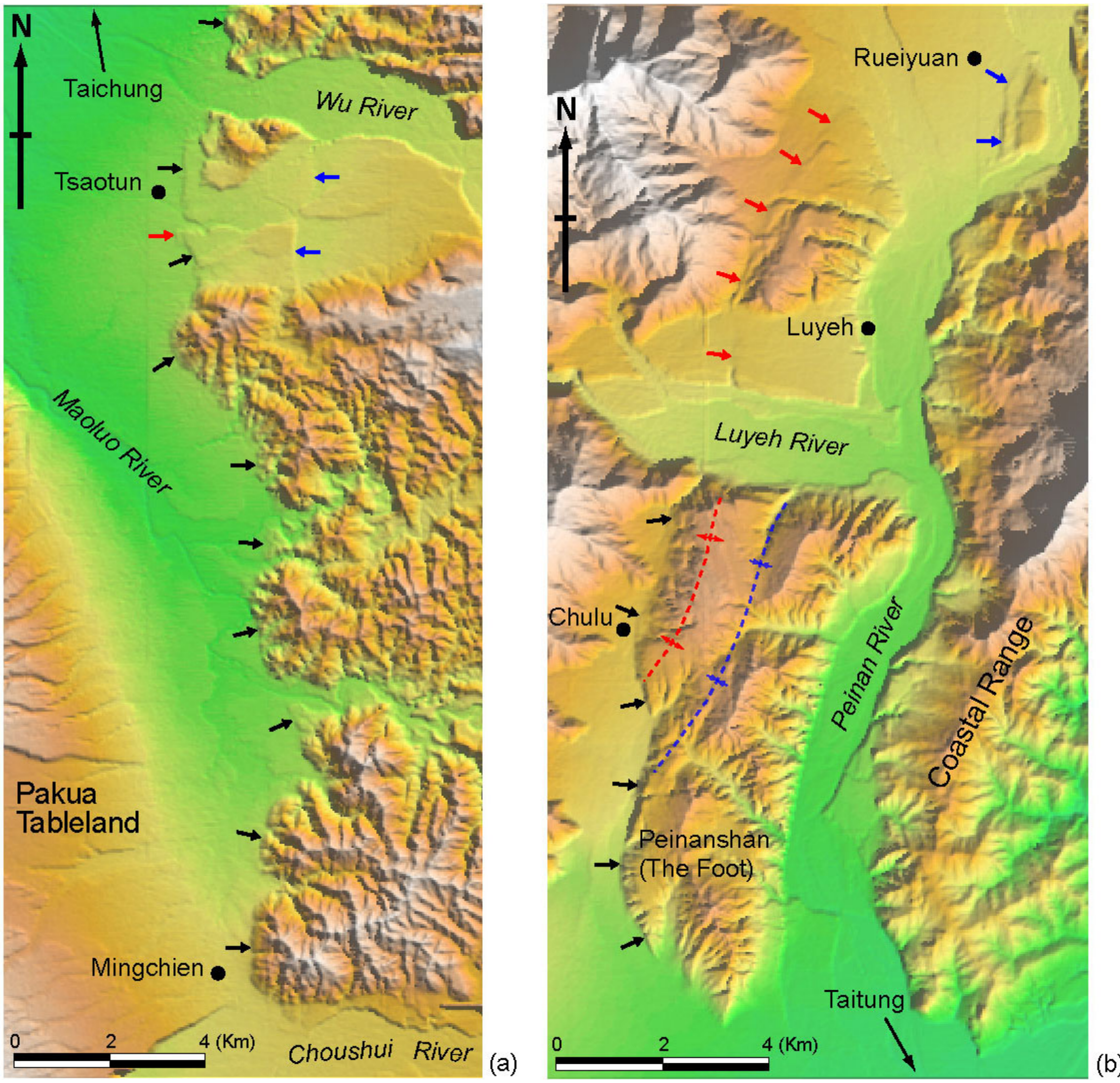
N
Taichung
Wu River
Tsaotun
Maoluo River
Pakua
Tableland
Mingchien
0
2
4 (Km)
Choushui River
(a)
Rueiyuan
N
Luyeh
Luyeh River
Chulu
Peinan River
Coastal Range
Peinanshan
(The Foot)
Taitung
0
2
4 (Km)
(b)

Figure 2

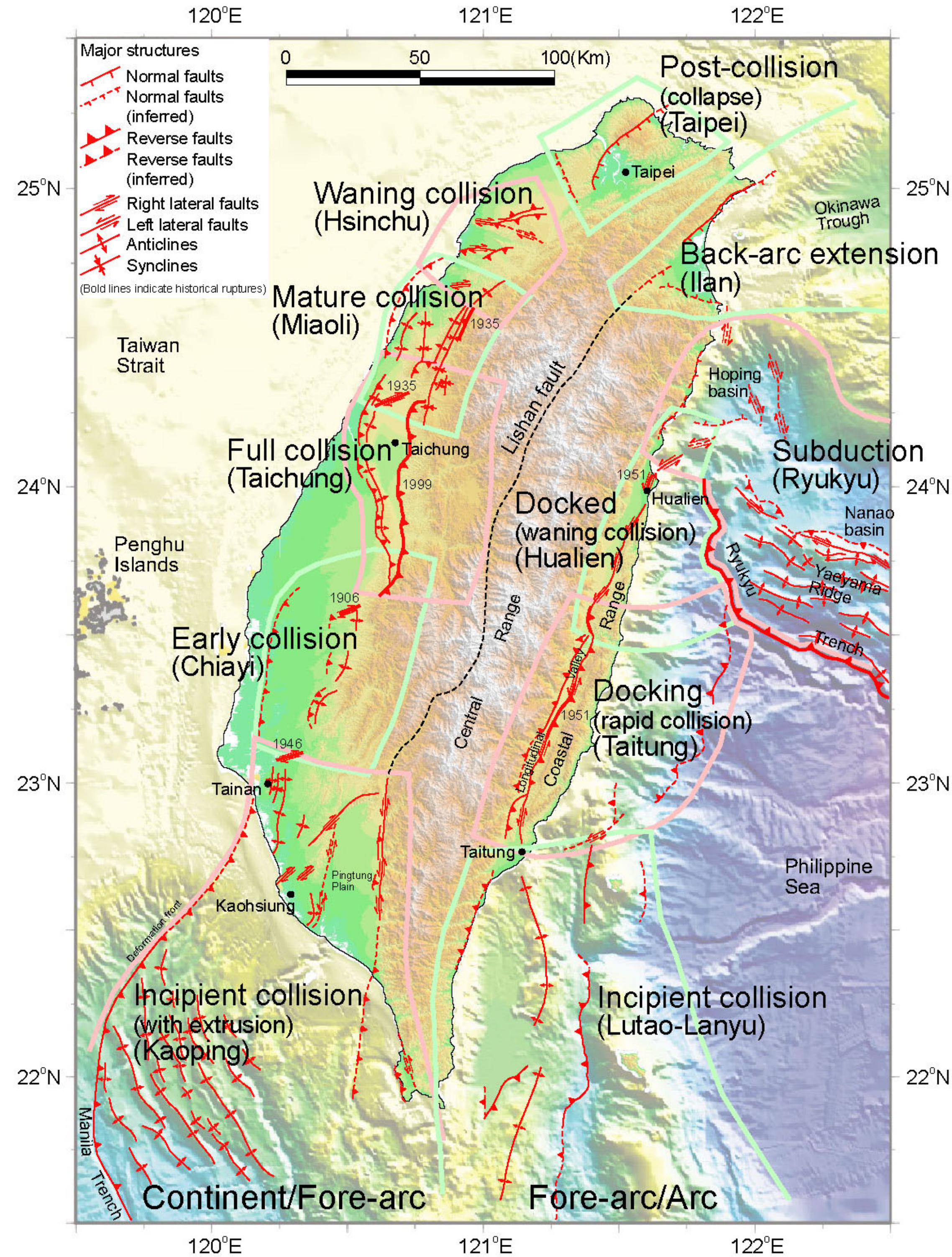

120°E
121°E
122°E
25°N
24°N
23°N
22°N
Major structures
Normal faults
Normal faults (inferred)
Reverse faults
Reverse faults (inferred)
Right lateral faults
Left lateral faults
Anticlines
Synclines
(Bold lines indicate historical ruptures)
0 50 100(Km)
Post-collision (collapse) (Taipei)
Taipei
Waning collision (Hsinchu)
Okinawa Trough
Back-arc extension (Ilan)
Mature collision (Miaoli)
1935
Taiwan Strait
Lishan fault
Hoping basin
Full collision (Taichung)
Taichung
1999
Subduction (Ryukyu)
1951
Hualien
Docked (waning collision) (Hualien)
Nanao basin
Penghu Islands
Ryukyu
Yaeyama Ridge
Trench
1906
Early collision (Chiayi)
Central Range
Coastal Range
Longitudinal Valley
Docking (rapid collision) (Taitung)
1946
Tainan
Taitung
Philippine Sea
Pingtung Plain
Kaohsiung
Deformation front
Incipient collision (with extrusion) (Kaoping)
Incipient collision (Lutao-Lanyu)
Manila Trench
Continent/Fore-arc
Fore-arc/Arc

Figure 3

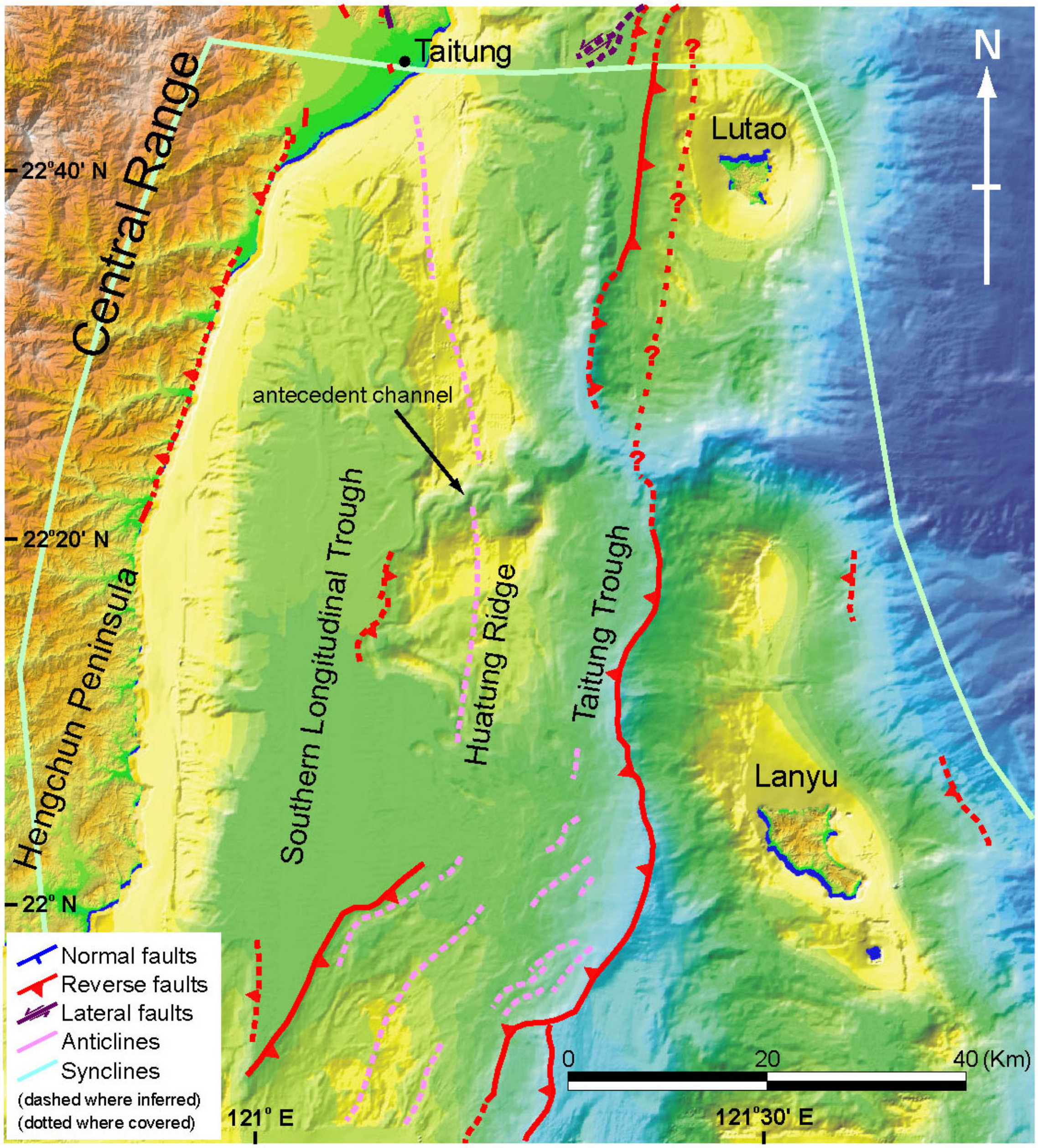
Taitung
N
Lutao
Central Range
22°40' N
antecedent channel
22°20' N
Hengchun Peninsula
Southern Longitudinal Trough
Huatung Ridge
Taitung Trough
Lanyu
22° N
Normal faults
Reverse faults
Lateral faults
Anticlines
Synclines
(dashed where inferred)
(dotted where covered)
121° E
0
20
40 (Km)
121°30' E

Figure 4

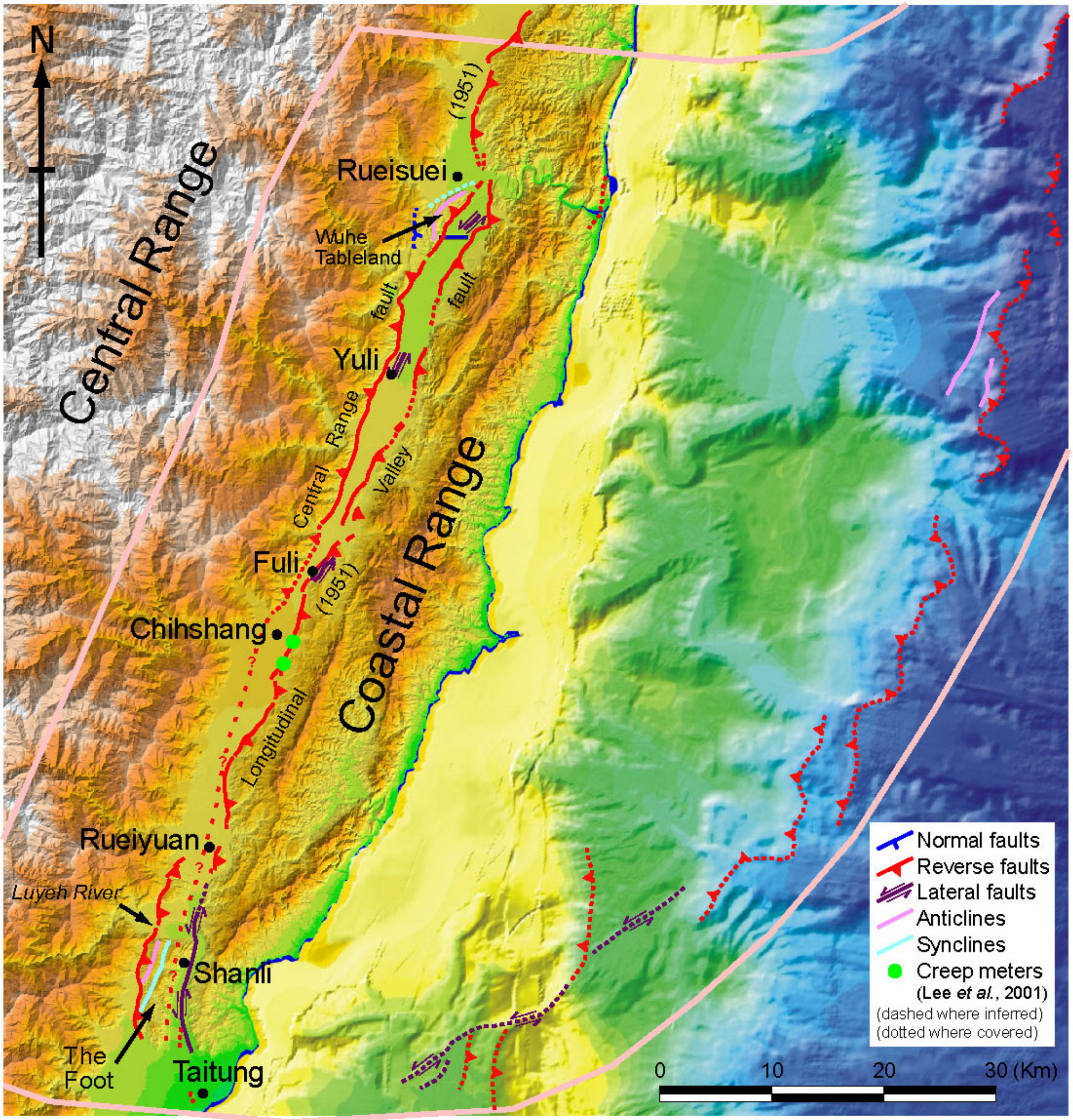
N
Central Range
Coastal Range
Rueisuei
Wuhe
Tableland
(1951)
fault
Yuli
Central
Range
Valley
Fuli
(1951)
Chihshang
Longitudinal
Rueiyuan
Luyeh River
Shanli
The
Foot
Taitung
Normal faults
Reverse faults
Lateral faults
Anticlines
Synclines
Creep meters
(Lee et al., 2001)
(dashed where inferred)
(dotted where covered)
0
10
20
30 (Km)

Figure 5

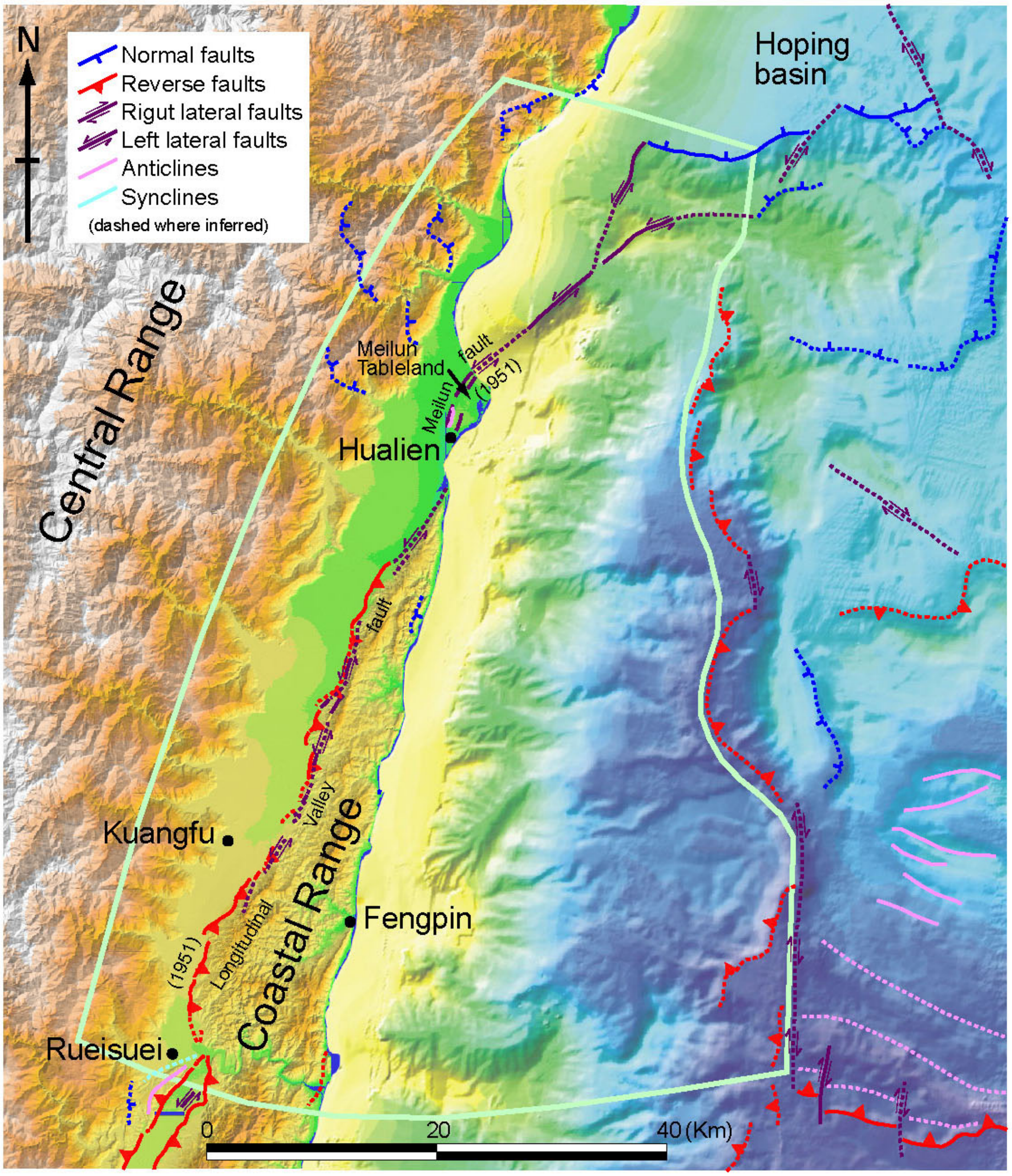
N
Normal faults
Reverse faults
Rigut lateral faults
Left lateral faults
Anticlines
Synclines
(dashed where inferred)
Hoping basin
Central Range
Meilun Tableland
Meilun fault
(1951)
Hualien
Valley
fault
Kuangfu
Coastal Range
Fengpin
Longitudinal
(1951)
Rueisuei
0
20
40 (Km)

Figure 6

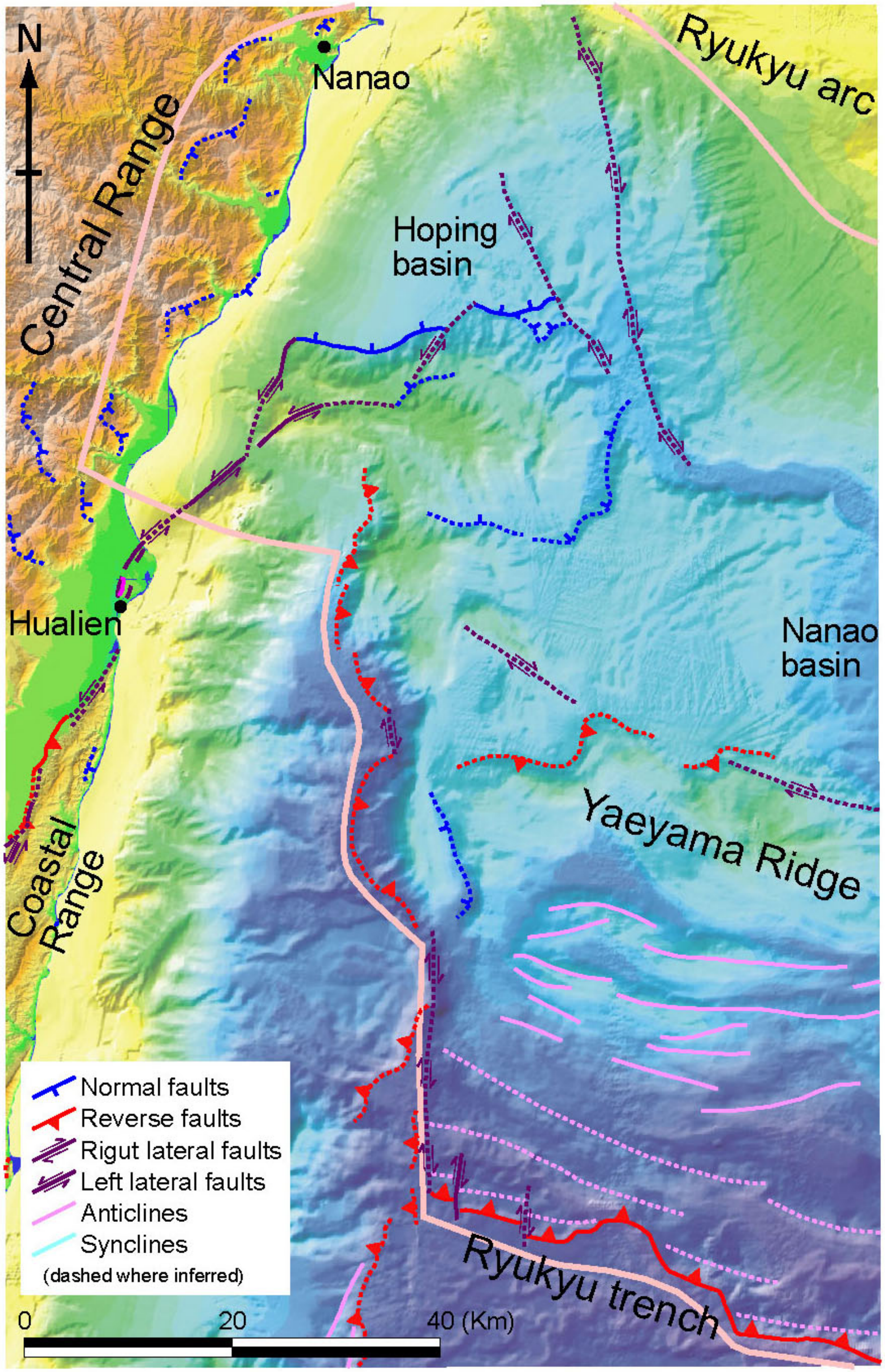
N
Nanao
Ryukyu arc
Central Range
Hoping
basin
Hualien
Nanao
basin
Yaeyama Ridge
Coastal
Range
Ryukyu trench
Normal faults
Reverse faults
Rigut lateral faults
Left lateral faults
Anticlines
Synclines
(dashed where inferred)
0
20
40 (Km)

Figure 7

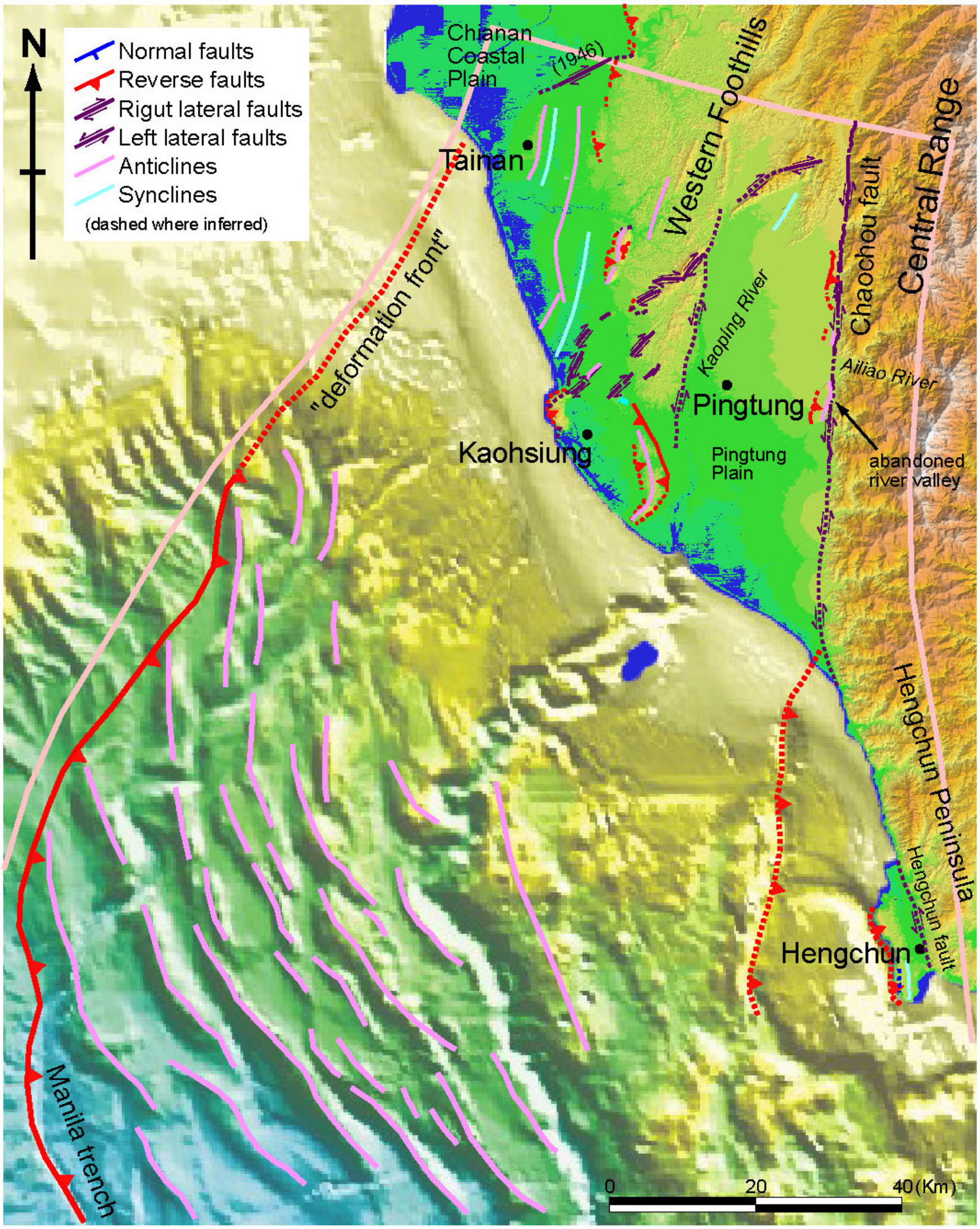
N
Normal faults
Reverse faults
Rigut lateral faults
Left lateral faults
Anticlines
Synclines
(dashed where inferred)
Chianan
Coastal
Plain
(1946)
Tainan
Western Foothills
Central Range
Chaochou fault
Kaoping River
Ailiao River
"deformation front"
Pingtung
Kaohsiung
Pingtung
Plain
abandoned
river valley
Hengchun Peninsula
Hengchun fault
Hengchun
Manila trench
0
20
40 (Km)

Figure 8

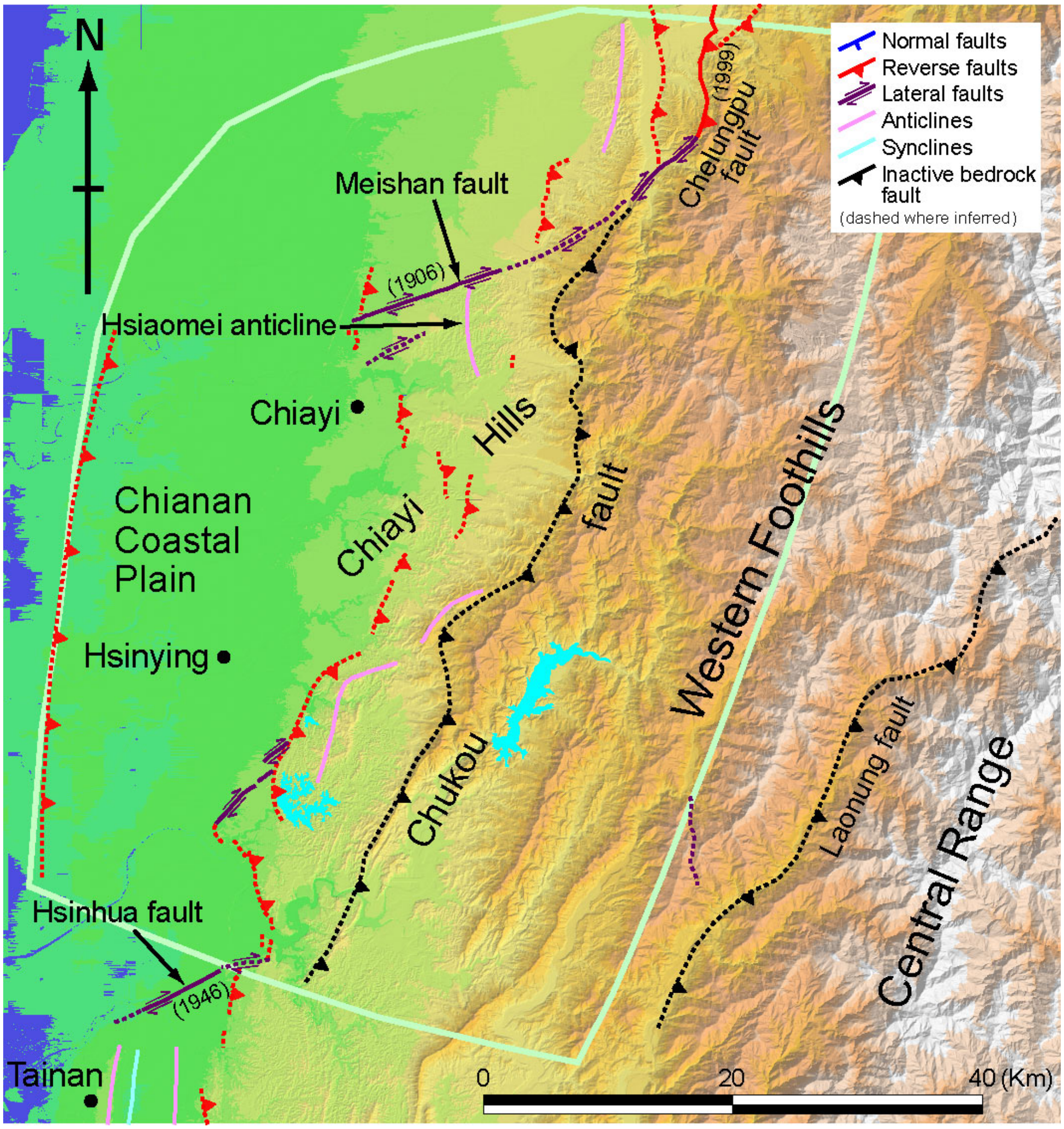
N
Normal faults
Reverse faults
Lateral faults
Anticlines
Synclines
Inactive bedrock fault
(dashed where inferred)
Meishan fault
(1906)
(1999)
Chelungpu fault
Hsiaomei anticline
Chiayi
Chiayi Hills
Chianan Coastal Plain
Hsinying
Chukou fault
Western Foothills
Laonung fault
Central Range
Hsinhua fault
(1946)
Tainan
0
20
40 (Km)

Figure 9

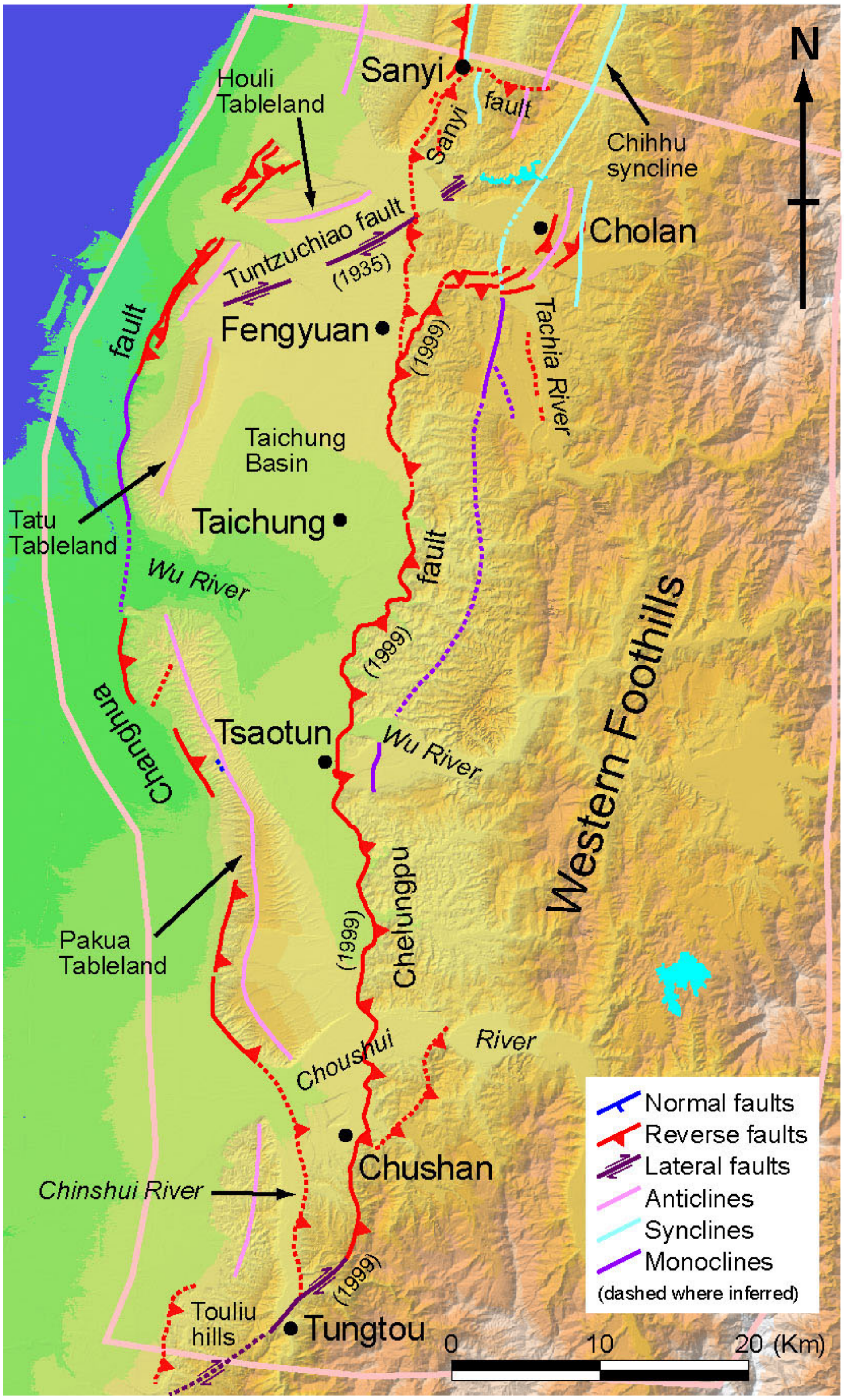
Sanyi
Houli
Tableland
Sanyi
fault
N
Chihhu
syncline
Cholan
Tuntzuchiao fault
(1935)
fault
Fengyuan
(1999)
Tachia River
Taichung
Basin
Tatu
Tableland
Taichung
Wu River
fault
Western Foothills
(1999)
Changhua
Tsaotun
Wu River
Pakua
Tableland
(1999)
Chelungpu
Choushui
River
Normal faults
Reverse faults
Lateral faults
Anticlines
Synclines
Monoclines
(dashed where inferred)
Chushan
Chinshui River
(1999)
Touliu
hills
Tungtou
0
10
20 (Km)

Figure 10

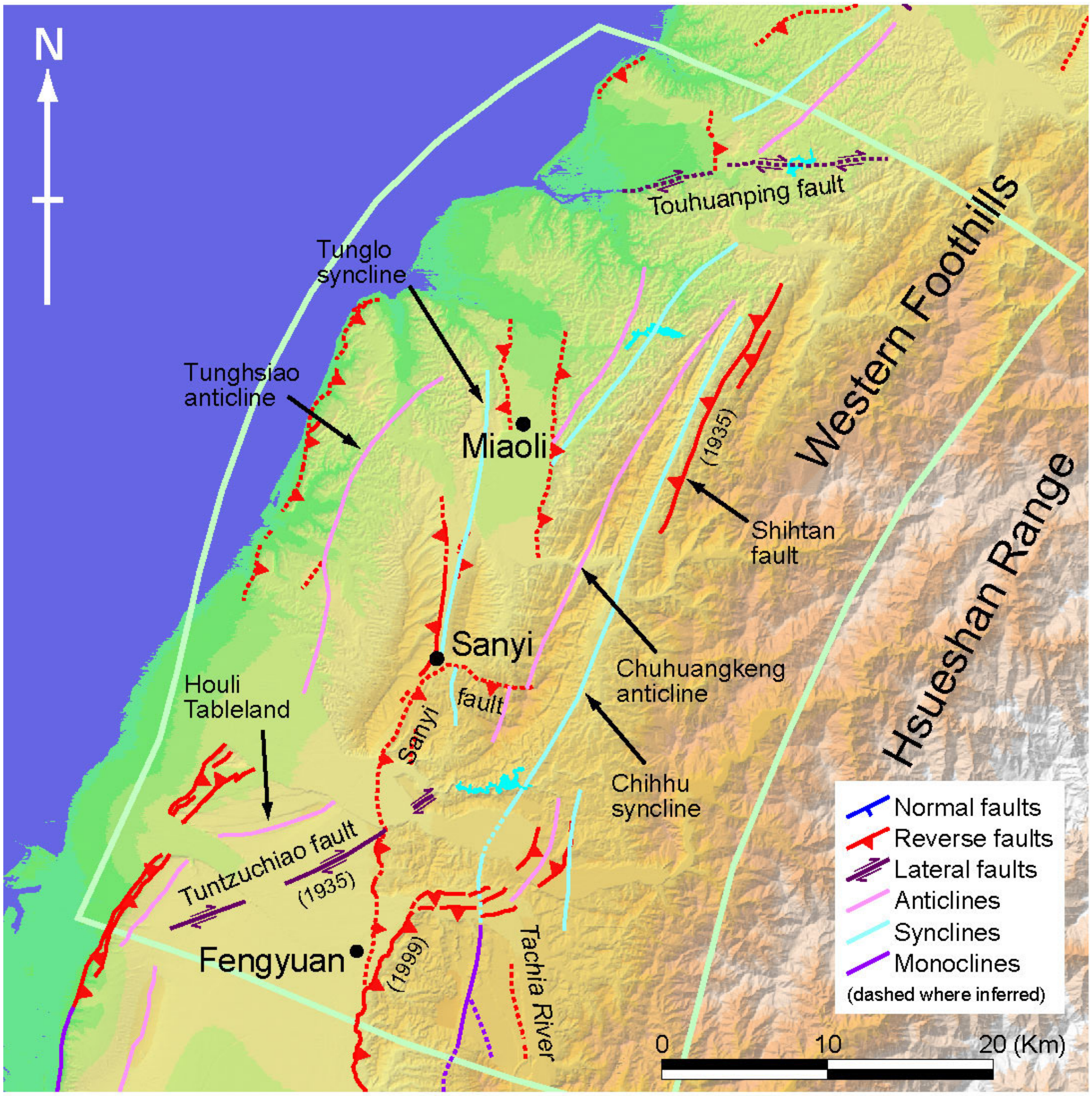
N
Touhuanping fault
Western Foothills
Tunglo syncline
Tunghsiao anticline
Miaoli
(1935)
Shihtan fault
Hsueshan Range
Sanyi
Chuhuangkeng anticline
Houli Tableland
Sanyi fault
Chihhu syncline
Tuntzuchiao fault
(1935)
Fengyuan
(1999)
Tachia River
Normal faults
Reverse faults
Lateral faults
Anticlines
Synclines
Monoclines
(dashed where inferred)
0
10
20 (Km)

Figure 11

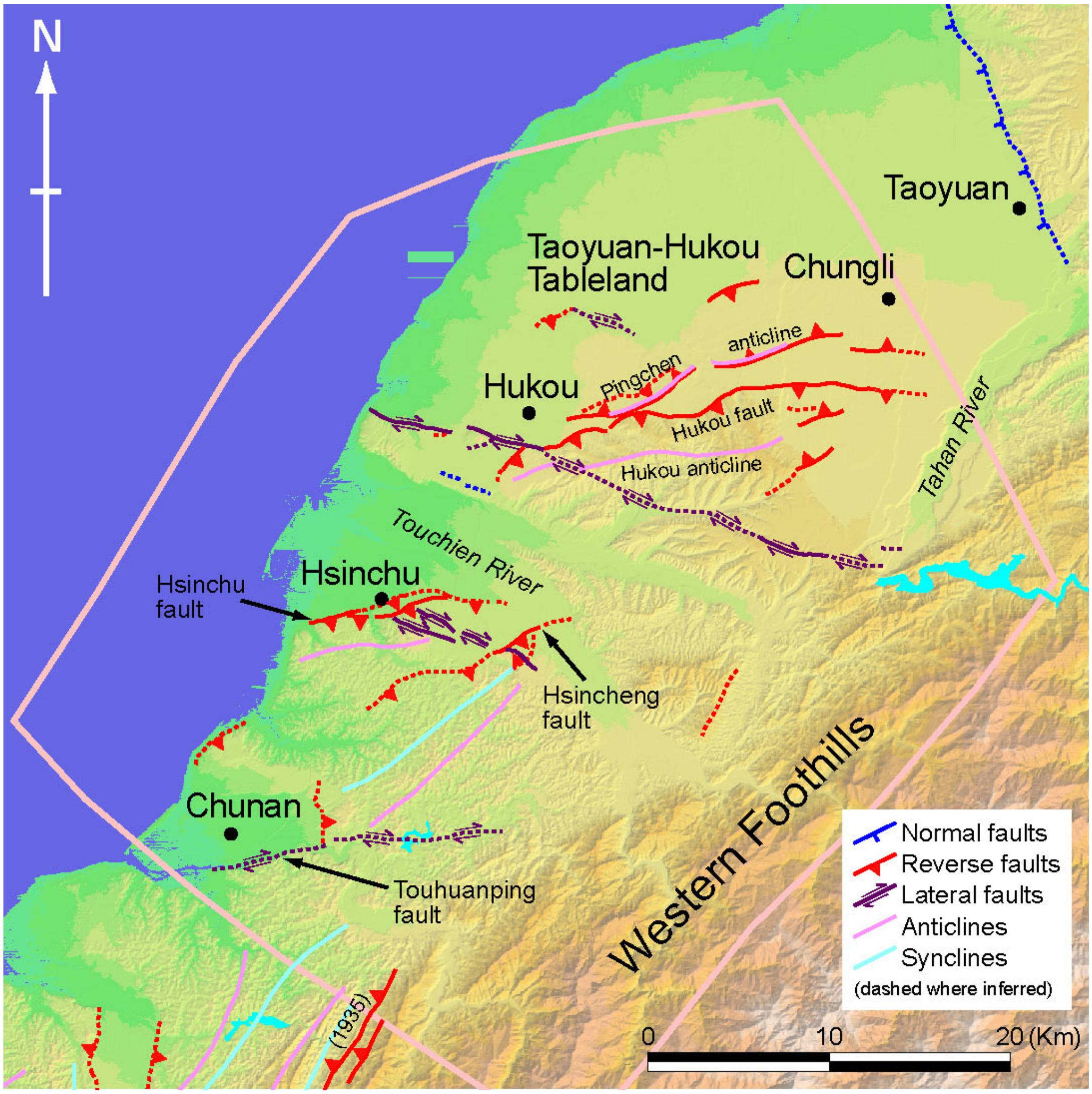
N
Taoyuan
Taoyuan-Hukou
Tableland
Chungli
anticline
Pingchen
Hukou
Hukou fault
Hukou anticline
Tahan River
Touchien River
Hsinchu
Hsinchu
fault
Hsincheng
fault
Chunan
Touhuanping
fault
Western Foothills
(1935)
Normal faults
Reverse faults
Lateral faults
Anticlines
Synclines
(dashed where inferred)
0
10
20 (Km)

Figure 12

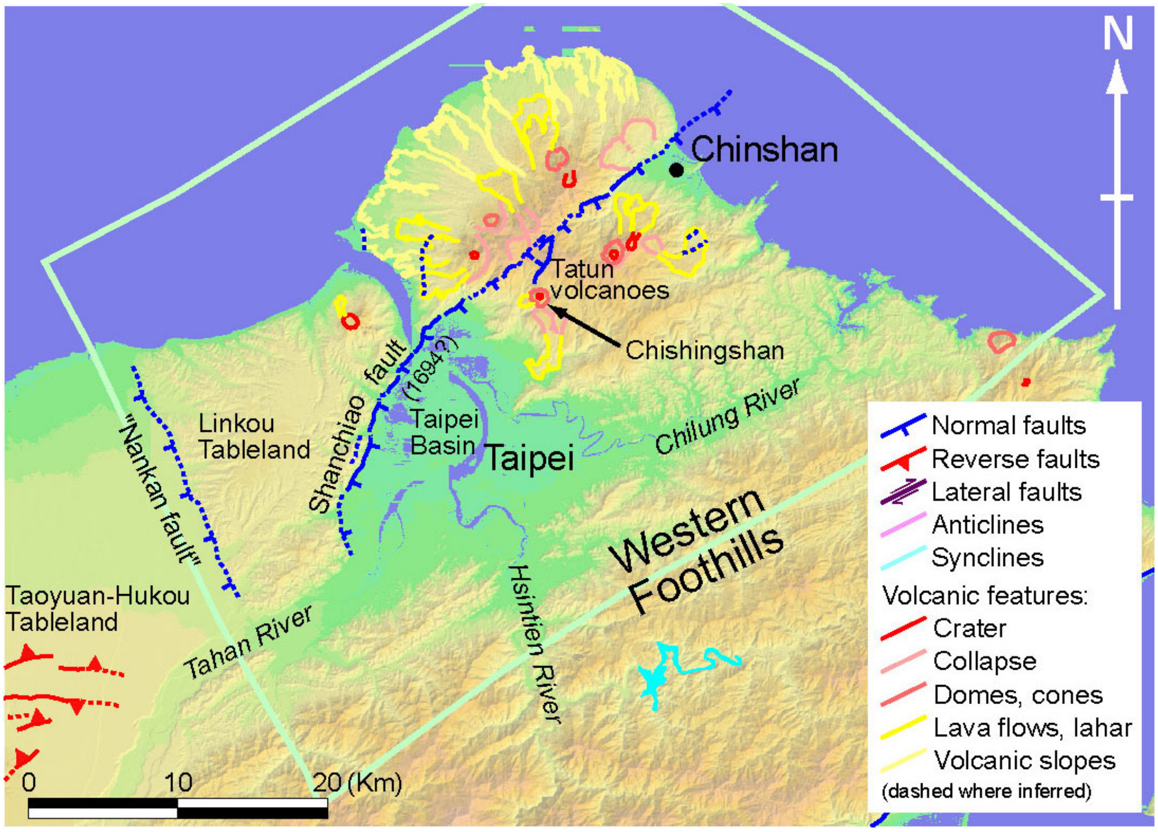
N
Chinshan
Tatun
volcanoes
Chishingshan
Shanchiao fault
(1694?)
Linkou
Tableland
"Nankan fault"
Taipei
Basin
Taipei
Chilung River
Western
Foothills
Taoyuan-Hukou
Tableland
Tahan River
Hsintien River
0
10
20 (Km)
Normal faults
Reverse faults
Lateral faults
Anticlines
Synclines
Volcanic features:
Crater
Collapse
Domes, cones
Lava flows, lahar
Volcanic slopes
(dashed where inferred)

Figure 13

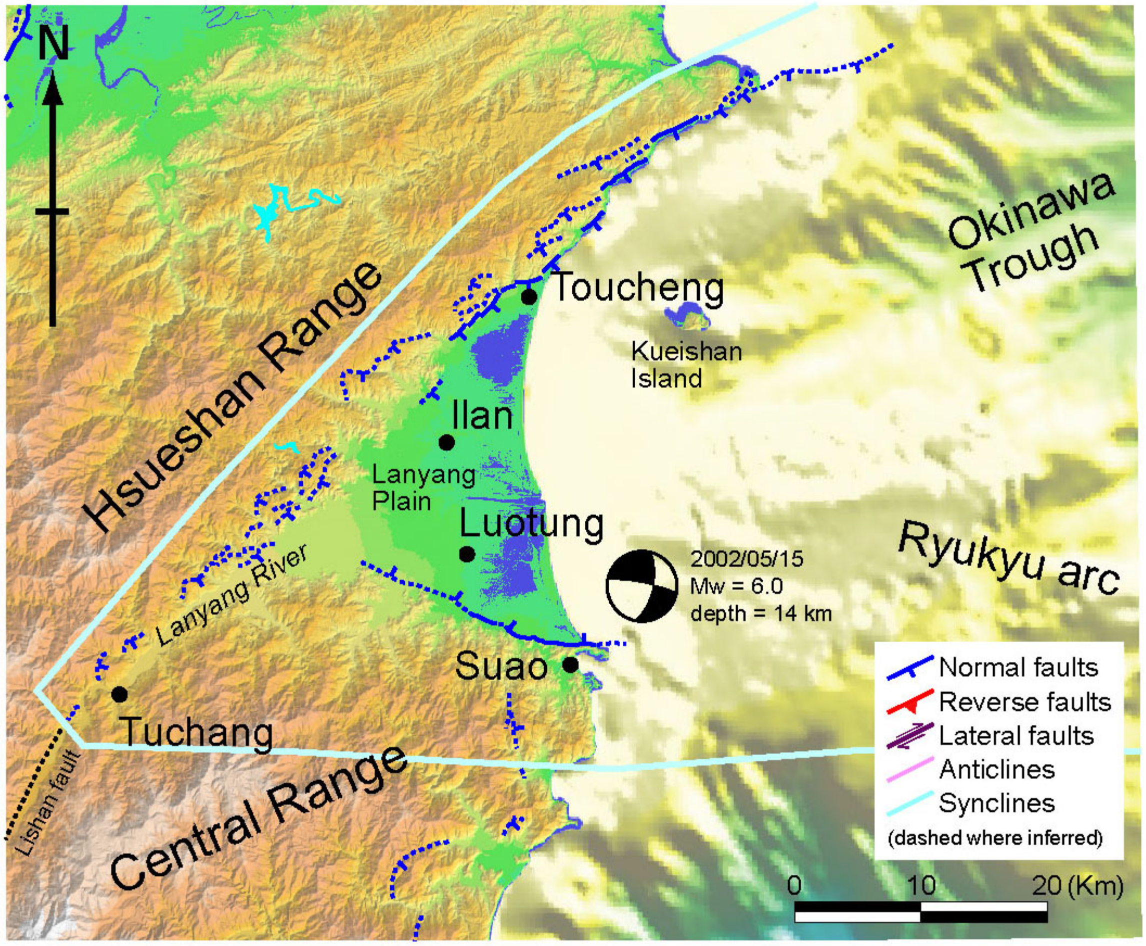
N
Hsueshan Range
Okinawa Trough
Toucheng
Kueishan Island
Ilan
Lanyang Plain
Luotung
Ryukyu arc
2002/05/15
Mw = 6.0
depth = 14 km
Lanyang River
Suao
Tuchang
Central Range
Lishan fault
Normal faults
Reverse faults
Lateral faults
Anticlines
Synclines
(dashed where inferred)
0
10
20 (Km)

Figure 14

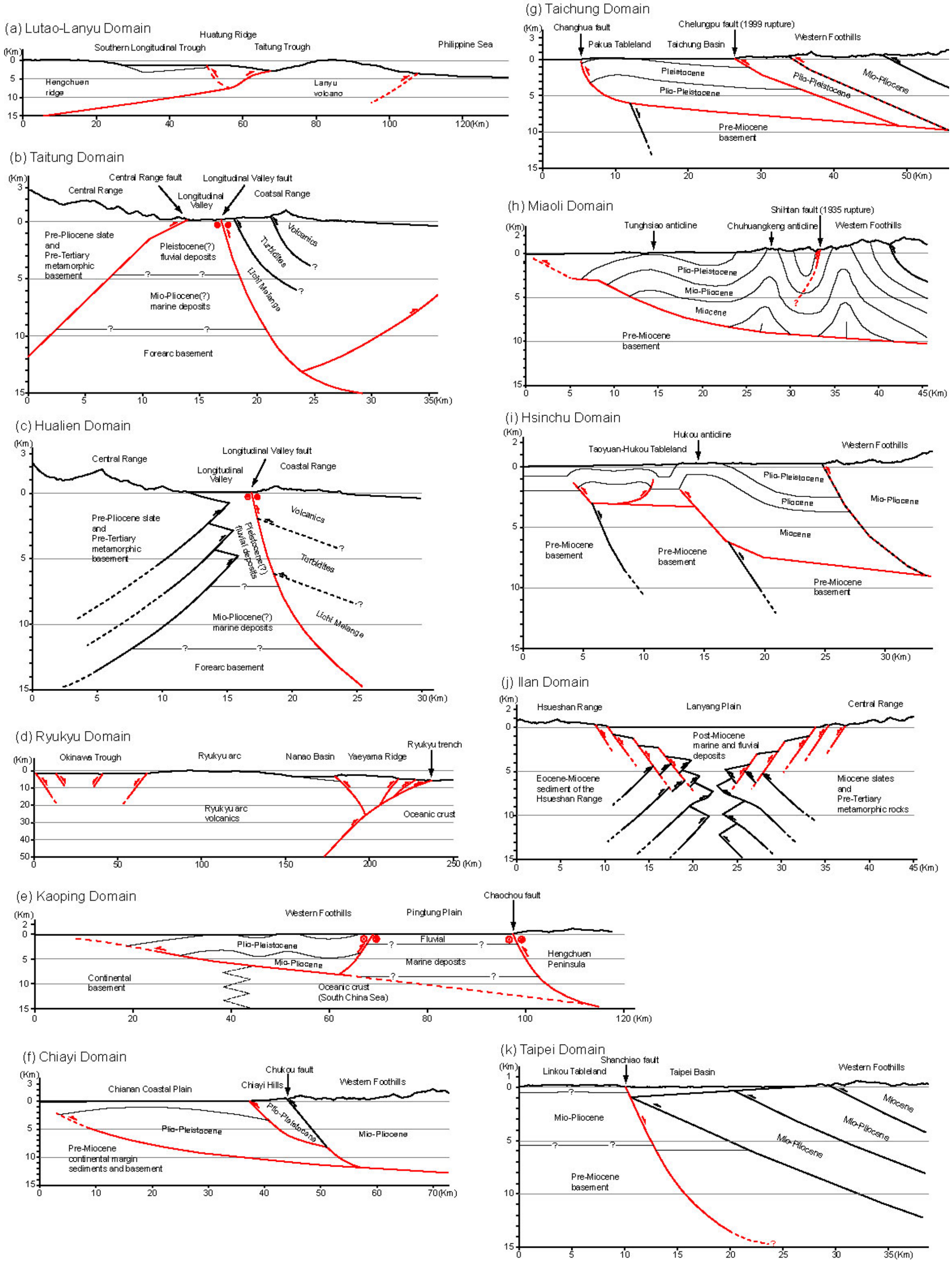

(a) Lutao-Lanyu Domain
Huatung Ridge
Southern Longitudinal Trough
Taitung Trough
Philippine Sea
Hengchuen ridge
Lanyu volcano
(b) Taitung Domain
Central Range fault
Longitudinal Valley fault
Central Range
Longitudinal Valley
Coatsal Range
Pre-Pliocene slate and Pre-Tertiary metamorphic basement
Pleistocene(?) fluvial deposits
Volcanics
Turbidites
Lichi Melange
Mio-Pliocene(?) marine deposits
Forearc basement
(c) Hualien Domain
Longitudinal Valley fault
Central Range
Longitudinal Valley
Coastal Range
Volcanics
Pre-Pliocene slate and Pre-Tertiary metamorphic basement
Pleistocene(?) fluvial deposits
Turbidites
Mio-Pliocene(?) marine deposits
Lichi Melange
Forearc basement
(d) Ryukyu Domain
Okinawa Trough
Ryukyu arc
Nanao Basin
Yaeyama Ridge
Ryukyu trench
Ryukyu arc volcanics
Oceanic crust
(e) Kaoping Domain
Chaochou fault
Western Foothills
Pingtung Plain
Plio-Pleistocene
Fluvial
Mio-Pliocene
Marine deposits
Hengchuen Peninsula
Continental basement
Oceanic crust (South China Sea)
(f) Chiayi Domain
Chukou fault
Chiayi Hills
Western Foothills
Chianan Coastal Plain
Plio-Pleistocene
Mio-Pliocene
Pre-Miocene continental margin sediments and basement
(g) Taichung Domain
Changhua fault
Chelungpu fault (1999 rupture)
Pakua Tableland
Taichung Basin
Western Foothills
Pleistocene
Plio-Pleistocene
Mio-Pliocene
Pre-Miocene basement
(h) Miaoli Domain
Shihtan fault (1935 rupture)
Tunghsiao anticline
Chuhuangkeng anticline
Western Foothills
Plio-Pleistocene
Mio-Pliocene
Miocene
Pre-Miocene basement
(i) Hsinchu Domain
Hukou anticline
Taoyuan-Hukou Tableland
Western Foothills
Plio-Pleistocene
Pliocene
Mio-Pliocene
Miocene
Pre-Miocene basement
(j) Ilan Domain
Hsueshan Range
Lanyang Plain
Central Range
Post-Miocene marine and fluvial deposits
Eocene-Miocene sediment of the Hsueshan Range
Miocene slates and Pre-Tertiary metamorphic rocks
(k) Taipei Domain
Shanchiao fault
Linkou Tableland
Taipei Basin
Western Foothills
Miocene
Mio-Pliocene
Pre-Miocene basement

Figure 15

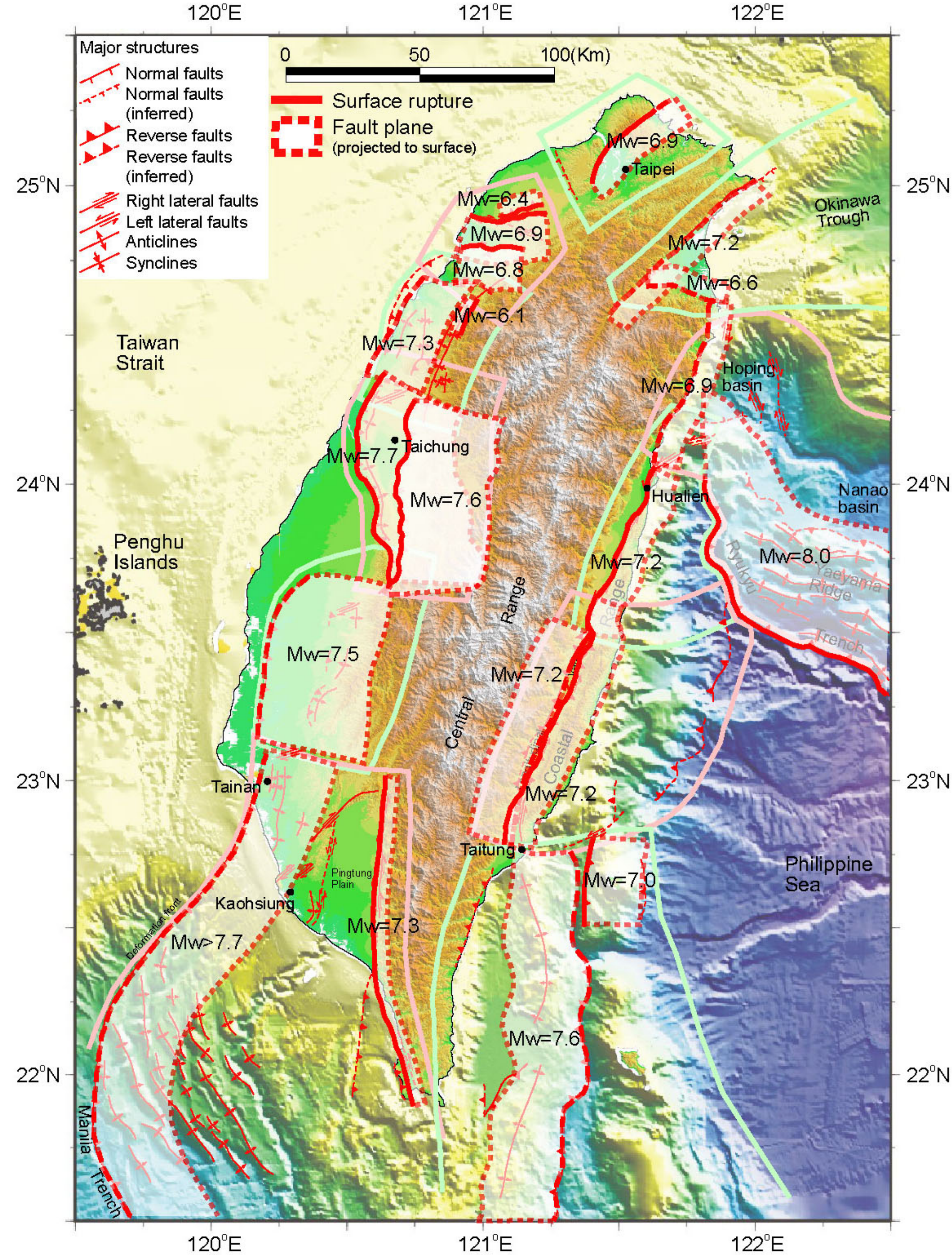

120°E
121°E
122°E
Major structures
Normal faults
Normal faults (inferred)
Reverse faults
Reverse faults (inferred)
Right lateral faults
Left lateral faults
Anticlines
Synclines
0
50
100(Km)
Surface rupture
Fault plane (projected to surface)
25°N
24°N
23°N
22°N
Mw=6.9
Taipei
Mw=6.4
Mw=6.9
Mw=6.8
Mw=7.2
Mw=6.6
Mw=6.1
Mw=7.3
Okinawa Trough
Taiwan Strait
Hoping basin
Mw=6.9
Taichung
Mw=7.7
Mw=7.6
Hualien
Nanao basin
Penghu Islands
Mw=7.2
Mw=8.0
Ryukyu
Yaeyama Ridge
Trench
Range
Mw=7.5
Mw=7.2
Central
Coastal
Tainan
Mw=7.2
Taitung
Philippine Sea
Pingtung Plain
Kaohsiung
Mw=7.0
Mw=7.3
Deformation front
Mw>7.7
Mw=7.6
Manila Trench

Figure 16